NATIONAL ACADEMY OF SCIENCES

Number 25 • July 1959

IGY BULLETIN

A monthly survey of programs and findings of the International Geophysical Year and the International Geophysical Cooperation-1959 as related primarily to United States programs.

Observation of Solar Cosmic Rays

The following material was prepared by P. S. Freier, E. P. Ney, and J. R. Winckler, of the School of Physics, University of Minnesota. A more detailed report was published in the Journal of Geophysical Research, *June 1959.*

A very unusual series of solar and terrestrial phenomena occurred in late March 1958, culminating in the arrival at the earth of low-energy cosmic rays. These events probably resulted from a solar flare of importance 3+ (the highest category of importance, indicating flares covering more than 1200 millionths of the sun's visible hemisphere); this flare began at 0950 UT, March 23, and ended about four hours later.

The flare was followed immediately by an extremely severe radio-noise storm on the sun. This storm produced radio emissions at all observed frequencies, from about 170 to 9400 megacycles, and a short-wave radio fadeout, which occurred between 0953 and 1309 UT, March 23. (J. F. Denisse, of Meudon Observatory, Paris, reported that at the lower frequencies the storm was one of the largest and longest ever recorded.)

The sudden commencement of a geomagnetic storm at 1540 UT, March 25, signaled the arrival at the earth of the cloud of solar gas presumably ejected by the flare. This was followed shortly by a pronounced decrease in cosmic-ray intensity at sea level.

Balloon Observations

High-altitude balloon data were obtained on the energy and composition of cosmic rays during the period of disturbance near Minneapolis (geomagnetic latitude 55°N). Balloon flights designated IGY 27, 28, and 29 were made on March 21 and 26 and on April 8, respectively. The balloons carried single counters and ion chambers, which record continuously the particle flux and the atmospheric ionization, and photographic emulsions for determining the precise nature of the particles involved.

Counting Rate and Ionization Intensity: Figure 1 presents the results of these measurements at an atmospheric pressure level of 10 millibars (about 102,000 ft). The ion-chamber curve shows constant and steady ionization on March 21 and a return to this condition by April 8. On March 26, however, the intensities measured by the single counter and ion chamber as the balloon reached peak altitude, at 1300 UT, were about 23% less than the March 21 values. This is consistent with the "Forbush decrease" in cosmic-ray intensity following a solar flare. (These decreases are now thought to indicate the modulating effect of the beam of solar particles on pre-exist-

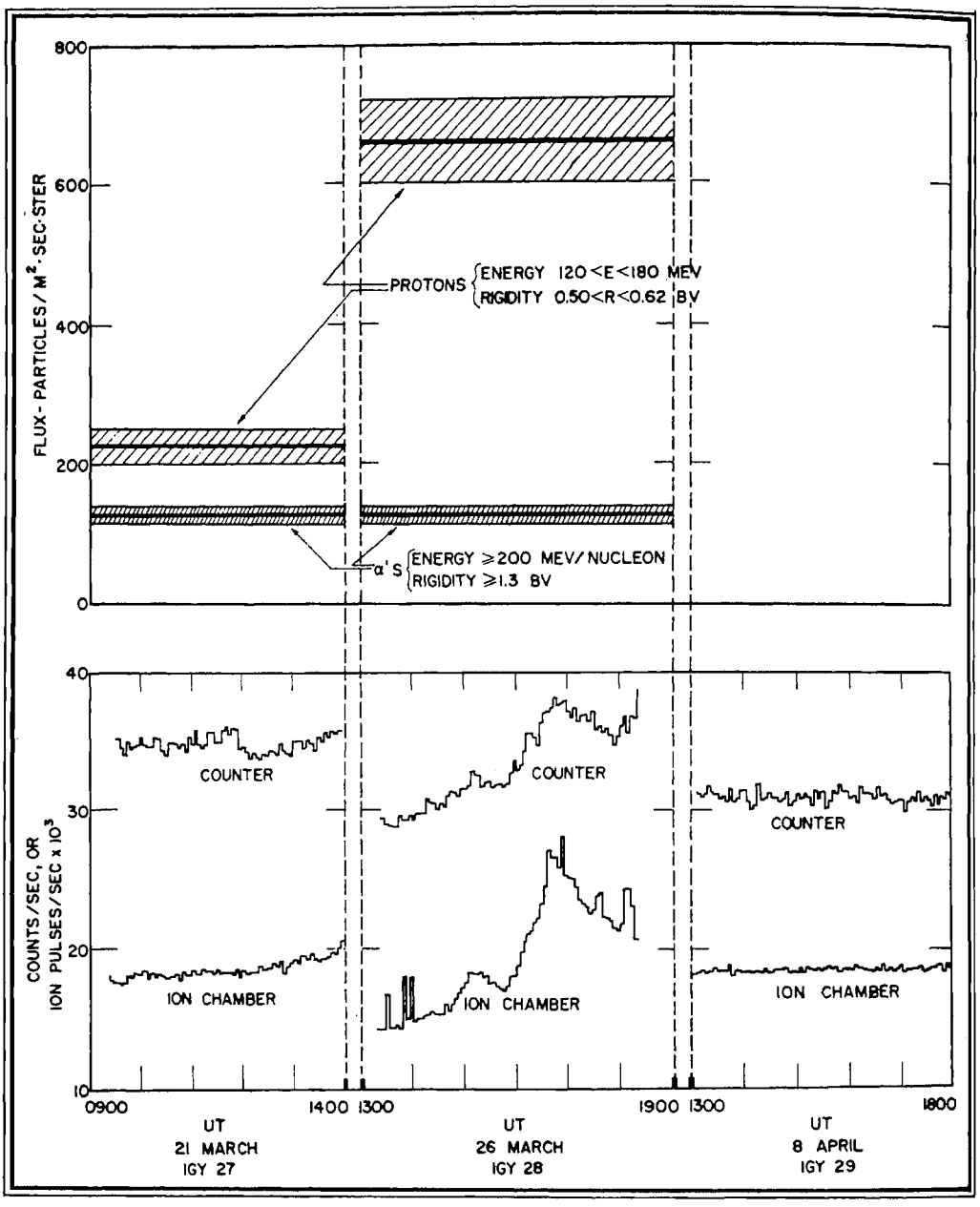

Fig. 1. *Counting Rates, Ionization, and Particle Composition as Measured on IGY Balloon Flights 27, 28, and 29. Upper part shows alpha-particle and proton flux measured by nuclear emulsions; lower part shows counting rates and ionization. The increase in ionization rate on March 26 agrees satisfactorily with the proton-flux increase shown by emulsions carried on the same flight.*

ing cosmic rays, causing a drop in intensity both at sea level and at high altitudes.)

On this occasion, the Forbush decrease was followed, about an hour after the balloon had reached ceiling altitude, by a slow *increase* in counting rate and in ionization. This continued throughout the remainder of the flight, a period of six hours. From

analysis of the ratio of ion-chamber to single-counter readings it was determined that if the ionizing particles were protons their range was 33 gms/cm^2 (i.e., they would penetrate any material to a thickness at which a cm^2 column would weigh 33 gms) and their energy was about 200 million electron volts (mev).

(It is possible that the increase with time of counting rate and ionization during the IGY-28 flight may actually represent a latitude effect, since the balloon drifted from Minneapolis to Sault Ste. Marie, Michigan. No increase was observed in a simultaneous flight in Texas, at geomagnetic latitude 41°N.)

Nature of Particles: Detailed studies were made to determine the nature of the particles associated with this increase in cosmic-ray intensity. The upper part of Figure 1 shows the results of observations of alpha particles (He^{++}) with energies greater than 200 mev/nucleon (equivalent to a total energy of 800 mev/alpha particle) and of protons (H^+) with energies of 120-180 mev. (Protons are believed to make up about 90% of primary cosmic rays, with heavier particles, including alpha particles, comprising the remainder.) The equipment used measured almost all alpha particles but only protons of rigidities between 0.50 and 0.62 BV. (Magnetic rigidity = momentum/charge, and is a measure of the resistance of the particle to deflection by a magnetic field; here, expressed in billions of volts, or BV.)

It was found that the flux of alpha particles of rigidity greater than 1.3 BV did not change measurably, but the flux of protons within the narrow rigidity range measured increased by the large amount of 0.04 particles/cm^2·sec·ster. At solar maximum, the total particle flux is about 0.1 particles/cm^2·sec·ster, i.e., 0.1 particles pass through a cm^2 area each second from directions lying within a three-dimensional angle of unit area, or steradian. The average increase in flux for the IGY-28 flight was, therefore, nearly half the total primary proton flux. This increase is consistent with the flux of protons of energies below 200 mev estimated from the ion-chamber to single-counter ratio, which was .06 particles/cm^2·sec·ster. During the event, protons arrived with rigidities as low as 0.5 BV, far below the rigidity cut-off of 1.0 BV for this geomagnetic latitude, inferred by P. Fowler, P. S. Freier, and E. P. Ney from previous direct-energy measurements. (Normally, only the higher-energy particles can penetrate the earth's magnetic field at the equator; lower-energy particles can penetrate only to certain geomagnetic latitudes, depending on their energies; very low-energy particles can penetrate only in polar regions.)

Sea-Level Intensity

A plot of sea-level neutron intensity at Deep River, Canada, March 20–April 10, is shown in Figure 2. In the period March 25–26 a drop in intensity of nearly 10% was measured, but it can be seen that the counting rate recovered from the decrease by early April. (These data were obtained by H. Carmichael.)

Cosmic-Noise Absorption

Data on the cosmic-noise absorption at Fort Yukon, Alaska, associated with the cosmic-ray phenomena described was supplied by H. Leinbach and G. C. Reid (Fig. 2, bottom). They report a very large absorption, amounting to 10 decibels, beginning abruptly on March 26 at the time of the sudden commencement of the magnetic storm. Even at night, on the nights preceding and following March 26, the absorption of cosmic noise was 3 db.

It is thought that this type of polar-cap cosmic-noise absorption may be caused by the arrival at the earth of charged particles, increasing ionization in the D-region of the earth's ionosphere. The particles appear to have been confined to the solar beam, since they were observed only when the earth entered the beam, at 1540 UT, March 25. The

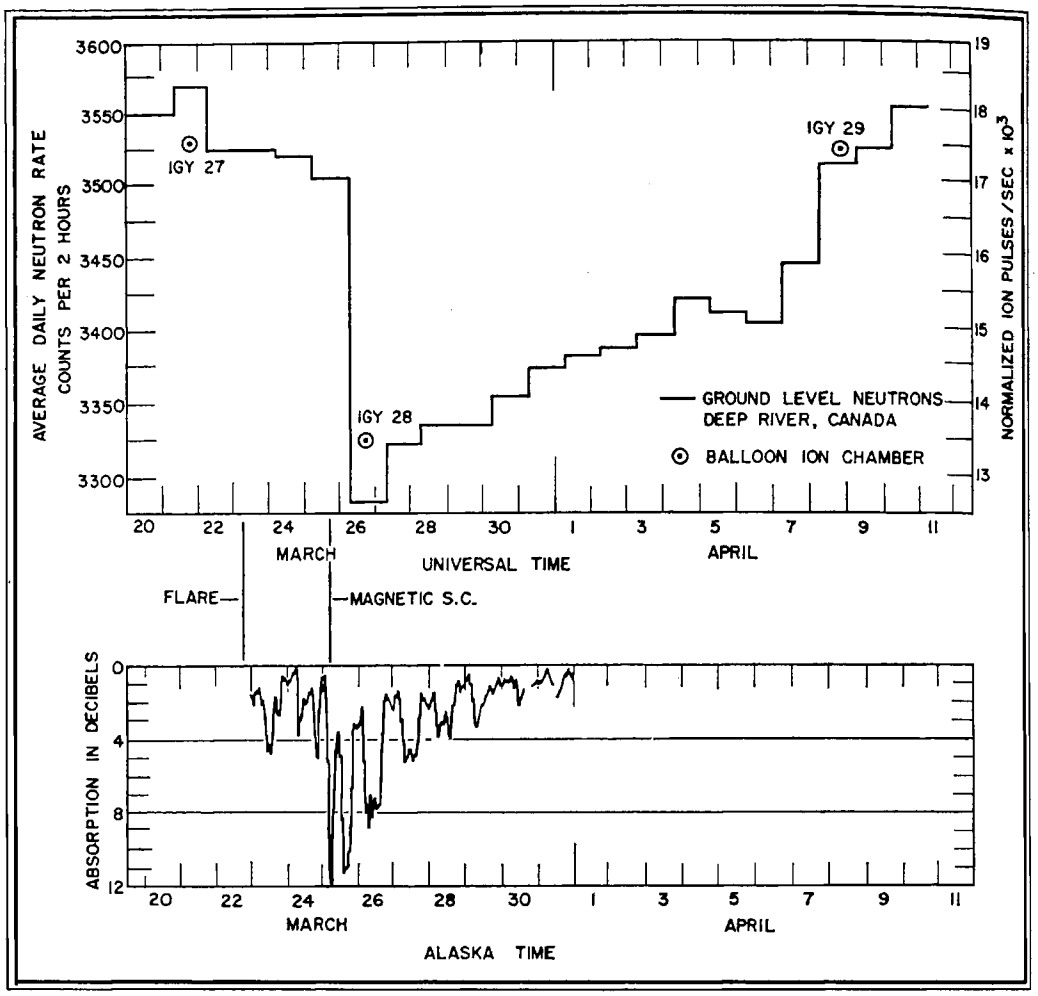

Fig. 2. *Sea-Level Neutron Intensity at Deep River, Canada, and Cosmic-Noise Absorption at Fort Yukon, Alaska. The neutron-intensity record also shows the total ionization rate at balloon ceiling altitude for IGY 27, 28, and 29.*

March 1958 disturbance may be the most intense event of this type observed up to that time.

(A second and even more intense event of this type was observed on May 11–12, 1959. The Minnesota investigators were informed by H. Leinbach that cosmic-noise absorption had reached 17 db on May 11. Accordingly, on May 11 and 12, five balloon flights were made. The observations showed that the May 11 event produced at least 50 times as many particles at balloon altitudes as were observed in the March event. In the more recent event, the solar beam apparently consisted almost entirely of protons.)

Conclusions

The significant features of this event are (1) the presence of particles with rigidities lower than the normal cut-off rigidity for the geomagnetic latitude of Minneapolis, and (2) the delayed arrival of cosmic rays following the solar flare of March 23.

The University of Minnesota investigators believe that the presence of low-rigidity

particles indicates distortion of the Stoermer cut-offs (the minimum particle energies needed to penetrate the geomagnetic field) by the solar beam ejected by the flare. They believe also that the late arrival of cosmic rays indicates storage in the solar corona of particles accelerated during the solar flare of March 23. The storage may have taken place between March 23 and March 30 and the particles may have arrived at the earth after being diffused into the magnetic channel associated with the solar beam.

Two other possible causes for the late arrival of the cosmic rays were considered: (a) The flare of March 23 produced a magnetic channel; subsequent solar activity accelerated the cosmic rays and injected them into the channel. This was ruled out because no major flares occurred in the period following March 23 to effect the acceleration and injection. (b) Particles trapped in the Van Allen radiation region (see *Bulletin No. 21*) were released by magnetic perturbation caused by the solar cloud. This was deemed improbable because of the polar-cap cosmic-noise absorption effects reported by Leinbach.

Rocket Studies of the Equatorial Electrojet

The following report is based on material supplied by Laurence J. Cahill, Jr., of the State University of Iowa. A more detailed account has been published in the Journal of Geophysical Research, *May 1959.*

Variations of the earth's magnetic field, long observed at the surface, are believed caused by electrical currents flowing in the ionosphere. However, the height, thickness, and current-density structure of these currents cannot be determined solely by ground-level measurements. Hence, the State University of Iowa included in its program of upper-atmosphere research the development of a small, light-weight magnetometer for use in rockoons. (*Bulletin No. 11* contains a brief description of the instrumentation and of the rockoon technique—which employs a balloon to lift a rocket to firing height.)

Successful flights were made during the IGY in both polar regions and in the mid-Pacific (Line Islands region), where the existence of the equatorial electrojet (see *Bulletin No. 17*) was further confirmed by direct measurements. This report is concerned with the equatorial electrojet studies.

The height and current density of the electrojet were measured at several latitudes during periods of magnetic calm and of moderate disturbance. In addition to the current layer previously predicted on the basis of ground-level measurements, another current layer was discovered slightly above the main electrojet current, and still another, flowing in the opposite direction, was found to the north.

The equatorial rockoon-magnetometer flights were made possible through the cooperation of Navy Task Force 43. SUI workers accompanied the USS *Glacier* on its cruise from Boston to the Antarctic during the Deep Freeze III expedition; in addition, the *Glacier* was allowed to deviate from its normal course for the Line Islands launchings and Navy personnel assisted with the launchings. Various SUI scientists, J. A. Van Allen in particular, supplied guidance and assistance in formulating the experiment, preparing the instrumentation, launching the rockoons, and reducing data.

Theory

The idea that variations in the earth's magnetic field observed at the surface are related to horizontal electric currents in the upper atmosphere is part of the "dynamo theory" of magnetic-field variations. In this theory, charged atmospheric particles are moved in tidal winds across the lines of force of the magnetic field, thus inducing electromotive forces in a direction perpendicular to the magnetic field. These electromotive forces cause positive and negative particles to move in opposite directions, setting up a system of electric currents in the atmosphere. Since the charged particles are provided by the horizontal ionospheric layers, the currents must likewise be principally horizontal. The tidal winds are related to the sun's movement across the sky; hence, the electrojet is primarily a day-time phenomenon.

The density of the electric current at any altitude above the surface depends on the velocity of the tidal winds producing the electromotive forces, the ionospheric conductivity at that altitude, and the strength of the magnetic field. Detailed information has in the past been lacking about the first two of these factors. Moreover, it seems likely that such information will for some time remain insufficient for detailed computation of the electric currents on the basis of the dynamo theory. However, the rocket magnetometer makes it possible to measure current densities directly and, along with electron-density measurements made by other rocket techniques, is supplying data which will help in computing conductivity more accurately.

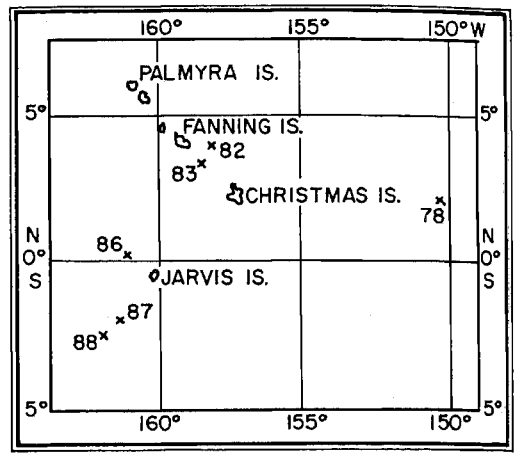

Fig. 3. *Location of Equatorial Electrojet Rockoon Flights, in the vicinity of the Line Islands.*

Flight Results

Six successful flights of the rocket magnetometer were made in the vicinity of the Line Islands (see Fig. 3 and Table 1). The records of three of these flights showed a normal approximate inverse-cube decrease with altitude in the intensity of the earth's magnetic field. The other three, flights 83, 86, and 87, apparently penetrated current layers in addition to recording the inverse-cube decrease.

The Scripps Institution of Oceanography established three ground-level magnetic ob-

Table 1. Flight Summary

Flight No.	(Oct. 1957) Date	Launching Time (at 165°W)		Location	Peak Alt. (km)
		Balloon	Rocket		
78	14	1216	1331	2°16′N, 150°23′W	113
82	17	1101	1216	3°56′N, 158°07′W	51
83	17	1244	1359	3°23′N, 158°41′W	127
86	18	1243	1356	0°02′N, 160°52′W	122
87	19	0750	0907	2°05′S, 161°05′W	129
88	19	1406	1519	2°31′S, 161°26′W	104

servatories in the Line Islands during the IGY to obtain new information about the equatorial electrojet through simultaneous observations at separate locations. These observatories supplied necessary information about the degree of magnetic disturbance during flights near them. Moreover, the rocket and ground-level measurements complemented each other: ground measurements supplied information on short and long-range changes in current intensity and on the location and periodic movements of the center of the current; rocket measurements provided a comparatively detailed picture of the extent in latitude and altitude of the electrojet and of its structure—the profile of current density with altitude.

East-West Current: Flight 83, in the electrojet region but somewhat to the north of the electrojet itself (Fig. 3), provided accurate and fairly complete data to a height of 125 kilometers, well into the ionosphere. The flight record shows an abrupt change of slope at 104 kilometers, indicating penetration of a current sheet. This slope change is a decrease, however; hence, the current must flow east-west in this region, directly opposite to the predicted direction of the equatorial electrojet. Since the flight curve resumes its original slope at 108 kilometers, the current sheet is rather thin. The record for the downward leg also shows the slope decrease at the same place that it appears on the upward-leg record, supporting the existence of this east-west current.

There is some evidence that this current is quite limited in lateral extent and would produce only very small ground-level effects, even in the absence of the masking effect of the more powerful electrojet.

Figure 4 is a plot of current density against altitude computed for part of flight 83, showing the east-west current layer detected during the flight.

Electrojet Flights: Flight 86 was launched 30 miles northwest of the Jarvis Island magnetic observatory at 1356 local time.

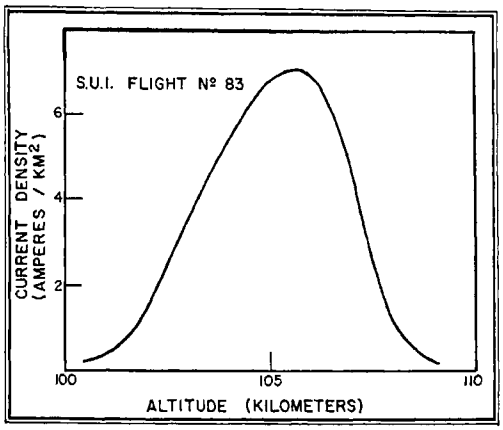

Fig. 4. *Current-Density Plot for Flight 83.*

Since ground-level measurements indicate that the electrojet appears to be closer to this observatory than to the others, it was expected that a launching at this location and time would result in penetration of the electrojet current.

The flight record shows an increase in slope at a height of 97 kilometers and a return approximately to the original slope at 110 kilometers, indicating that the rocket had passed through the electrojet in this region. (A rocket flight made during studies conducted by S. F. Singer and others in 1949 also entered the electrojet at approximately the same height.) Detailed plots of the flight record, however, reveal that above 110 kilometers the slope does not return entirely to its value at lower levels and that it again increases near 117 kilometers. Thus, two distinct current layers are indicated, with a layer of lower current density between them. Since the slope does not return completely to the lower-level value at the peak altitude reached by the rocket, 122 kilometers, the upper layer evidently was not completely penetrated.

The records for flight 87, southwest of Jarvis Island, also indicate penetration of the two current layers. The lower layer was found to be at the same altitude as in flight 86, but the upper layer was slightly higher. The current intensities were found to be

much greater on flight 87 than in the previous flight. There is some inconclusive evidence that the upper layer may have been penetrated completely near the peak altitude of this flight, 129 kilometers. Figure 5 is a plot of current density against altitude for flight 87.

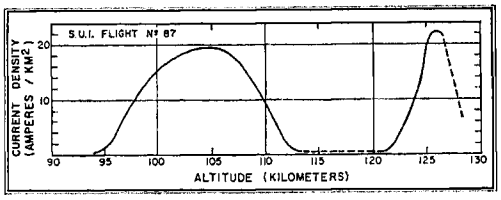

Fig. 5. *Current-Density Plot for Flight 87. Note two peaks, representing upper and lower current layers of electrojet.*

Intensity and Structure of Electrojet

Records from flights 83, 86, and 87, taken together with corresponding records from the Line Islands observatories, were used to sketch the intensity and structure of the equatorial electrojet.

Intensity: The departure from the normal inverse-cube decrease at the peak altitude of flight 86 was 138 ± 10 gamma (γ). (The sea-level magnitude of the earth's magnetic field at the equator is 34,000γ.) The contribution of the current sheet to the daily magnetic variation at sea level, as estimated from the rocket measurements, is 59 ± 4γ. This value, although in excellent agreement with the ground-level measurements, is surprising since the upper current layer was not completely penetrated. It is thought that only ⅔ of the value of the daily variation at sea level is attributable to the overhead current sheet (the Jarvis value was 90 ± 6γ at the time of the flight).

On flight 87, the total departure from the normal inverse-cube decrease at peak altitude was 300 ± 20γ, slightly more than twice that measured on flight 86. The expected contribution to the daily surface variation in this region is 127 ± 9γ, which does not agree with the value based on surface measurements (137 ± 4γ, or ⅔ the total measured value of 206 ± 6γ) quite as well as in the previous flight. This may be because ground measurements of overhead currents in the Jarvis region at the time of flight 87 indicated they were more intense than those found by rockets in the vicinity of flight 87, about 120 miles farther south.

Variograph records of the vertical component of the magnetic field (F) from Palmyra and Jarvis indicate local regions of more intense current imbedded in the electrojet. Although the main daily variation in F at these stations is similar, small, temporary fluctuations are opposite in phase. This indicates that the source of these small fluctuations lies between Jarvis and Palmyra. The center of the electrojet, however, appears to be south of Jarvis.

The currents measured up to heights of 129 kilometers appear to be of sufficient magnitude to account for all of the ground-level daily variations. However, it is believed there may be additional current layers above the peak rocket altitudes reached. Such currents might be too weak to produce observable variations at the ground, or they could be in pairs flowing in opposite directions, cancelling out each other's effects.

Structure: Figure 6 is a vertical cross-section of the equatorial electrojet based on extrapolations from the available experimental data. It is intended only as a graphic portrayal of the data and not as a precise or reliable picture of the actual electrojet.

The total width of the electrojet is estimated at about 300 kilometers, with the northern boundary lying between the sites of flights 83 and 86. (The width estimate agrees with a ground-level latitude survey by C. A. Onwumechilli, of the University of Nigeria, and with electrojet conductivity calculations by D. F. Martyn.) Flights 86 and 87, as well as earlier measurements by Singer and others, fix the bottom of the lower electrojet layer at a height of 97 kilo-

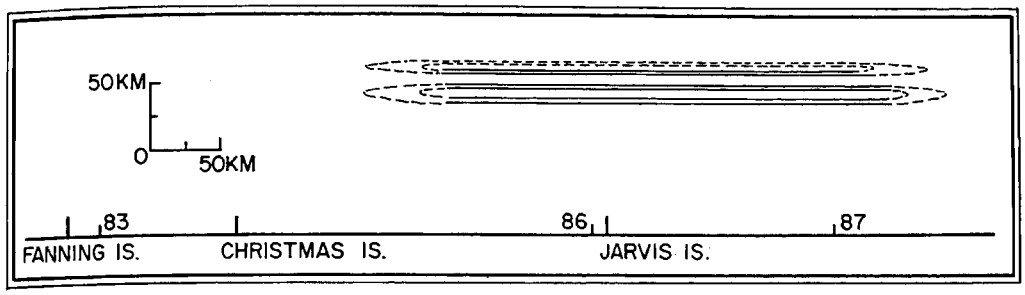

Fig. 6. *Cross-Section Showing Approximate Structure of Equatorial Electrojet. Inner lines represent regions of higher current density; numbers at bottom are flight numbers at their positions relative to the electrojet.*

meters. The top of the lower layer is at about 110 kilometers.

The lines within the layers in Figure 6 represent current-density regions, with density increasing toward the center of the layer. (Actual current densities vary daily and from day to day, and, as already mentioned, local regions of higher density may be present.) The altitude and thickness of the upper layer, as well as the interval between the two layers, appears to be variable.

Variations in the intensity and height of the upper layer may be related to the degree of magnetic disturbance or to several other factors, such as season, time of day, or phase of the moon. The flights described were made on both magnetically disturbed and on magnetically quiet days, shortly before the autumnal equinox, and when the moon was in the last quarter.

The presence of two current layers at the equator, rather than the single layer predicted from ground studies, must still be explained. A possible explanation is the presence of a high-electron-density layer above the altitude of peak ionospheric conductivity (near 100 kilometers). An intense sporadic-E reflection has been observed near the magnetic equator in the same region as the electrojet. (Sporadic-E refers to clouds, or patches, of ionization in the E-region of the ionosphere which reflect radio waves.) This sporadic-E layer could be responsible for one of the current layers, but which current layer might be due to the sporadic-E and which might be due to the peak in conductivity is not yet clear.

Antarctic Traverse Reports

Related materials from two sources bearing on the possible existence of a trans-Antarctic trough, along with other traverse findings, are presented in the following report. The first part of the report is based on a paper given at the May 1959 meeting of the American Geophysical Union (AGU) by Edward Thiel and Ned A. Ostenso. The second part is based on a paper presented by Charles R. Bentley and Ostenso at the same meeting. In both cases, the material was prepared at the University of Wisconsin.

I. AIRBORNE TRAVERSE, 1958–59

A principal result of the first season of IGY Antarctic oversnow traverse activity was the discovery that the Filchner Ice Shelf, which borders the Weddell Sea, extends much farther inland than had previously been supposed. Beneath its eastern

part, seismic sounding revealed a trough in the ocean floor, the axis of which averaged 1100 meters below sea level. This trough was still evident when crossed by the Ellsworth traverse party for the last time at 82°S, some 300 miles inland from the front of the shelf.

These findings reopened the question of whether the Antarctic continent is divided by a down-warped, ice-filled depression connecting the Ross and Weddell Seas.

The airborne traverse followed a path at right angles to the hypothetical trough. Traveling in a Navy aircraft, the three-man scientific team made seven landings along meridian 130°W. They covered some 400 miles between the Harold Byrd Mountains and the Executive Committee Range. (See Fig. 7.)

Geographic positions were determined by solar navigation, surface elevations by altimetry, and ice thicknesses by seismic sounding. Gravity observations were made throughout, to indicate ice thickness in the event areas were encountered in which no suitable seismic reflections could be obtained, and to provide information on the type of underlying rock. Shallow pit studies and coring determined the mean annual temperature and snow accumulation, and magnetic declinations were measured. Three hours' work was required at each station.

The seismic program at each station consisted of a vertical sounding for ice thickness, and of small explosions at each end of a 330-meter cable on the ice surface; the cable contained 12 geophones, equally spaced, to determine the average seismic-

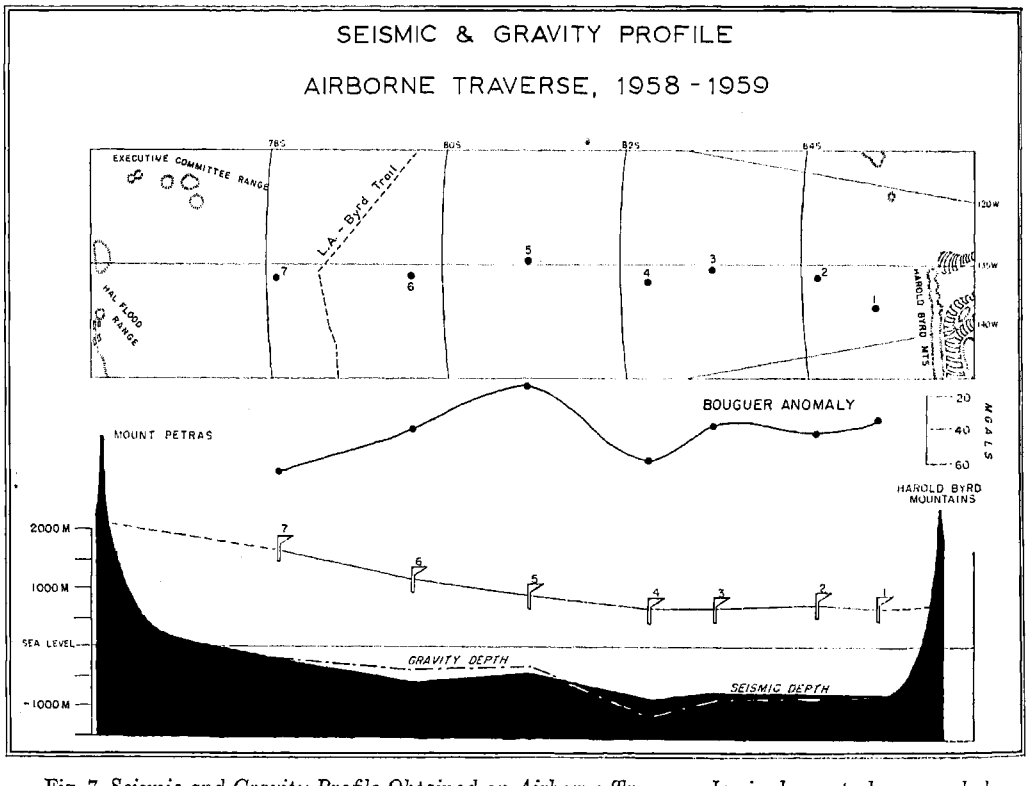

Fig. 7. *Seismic and Gravity Profile Obtained on Airborne Traverse. Ice is shown to be grounded at all seven stations between the mountain ranges, lending support, in this region, to the thesis of a connection between the Ross and Weddell Seas in the form of a down-warped, ice-filled trough.*

wave velocity for the ice column. Good reflections were obtained at five stations; those at the other two were usable but of poorer quality, perhaps because of nearness to crevassed areas.

Figure 7 contains a profile presenting the results of this seismic program. Since the ice is shown to be grounded at all seven stations between the mountain ranges at either end of the line, there appears to be virtually no possibility of water interchange between the Ross and Weddell Seas. However, the profile does appear to support the thesis of a down-warped, ice-filled trough connecting the two seas. Nevertheless, additional data, especially on the area to the east, are needed.

Related Results

Some further light is thrown on the trough problem by data so far available from the Marie Byrd Land oversnow traverse of 1958–59, which was in the field at the same time as the airlifted group. (This traverse is discussed in more detail in Part II, where it is referred to as the Horlick Traverse.) It traveled a triangular path: leg A, from Byrd Station across the hypothetical trough region to the foot of the Harold Byrd Mountains; leg B, eastward roughly paralleling the great trans-Antarctic range; and leg C, back to Byrd Station, once again crossing the trough region.

Leg A produced results similar to those found by the airborne party along 130°W —grounded ice resting on a rock surface below sea level. Over much of leg B the buried rock surface was found to be above sea level; this is not surprising since it paralleled the mountains to the south of the axis of the hypothetical downwarp. On the southern half of leg C the buried rock surface was found to be above sea level, with the important exception of a 40-mile gap where the rock descended to 1000 meters below sea level. Since the rock surface below Byrd Station is known to lie 1000 meters below sea level, any trough must pass through or near the Byrd Station area, or through the 40-mile gap found on leg C. (An earlier figure of about 1500 meters, or 5000 feet, for depth of the rock surface in the Byrd Station area has been corrected to 1000 meters, based on additional data and computations.)

To help determine whether such a trough actually extends across the continent or whether it is broken by a land bridge under the ice between the South Pole region and the Palmer Peninsula Mountains bordering the Weddell Sea, an airborne traverse along the 88°W meridian between the Horlick and Sentinel Mountains has been proposed for the coming Antarctic field season. This area is considered the most likely for such a connection because of its isolated nunataks and high snow surface.

II. MARIE BYRD LAND TRAVERSES

Study has been carried out to date on the results of three oversnow traverses in Marie Byrd Land. The first (Fig. 8) followed the pre-established trail from Little America Station to Byrd Station during the month of February, 1957. The second, or Sentinel, traverse proceeded clockwise around a loop to the northeast of Byrd Station between November 19, 1957, and February 19, 1958. The third (Horlick) traverse lasted from November 1, 1958, to January 20, 1959, and covered, in a counter-clockwise direction, a loop south of Byrd Station.

On all traverses, seismic reflection shooting was carried out at intervals of about 30 nautical miles, with gravimetric, magnetic, and altimetric measurements every three miles. Reflection shooting was supplemented by a large number of short refraction measurements in which the variations of seismic-wave velocities in the upper 50 meters of firn were studied, and by eight long refraction profiles which produced information concerning velocities throughout the icecap and in the rock beneath.

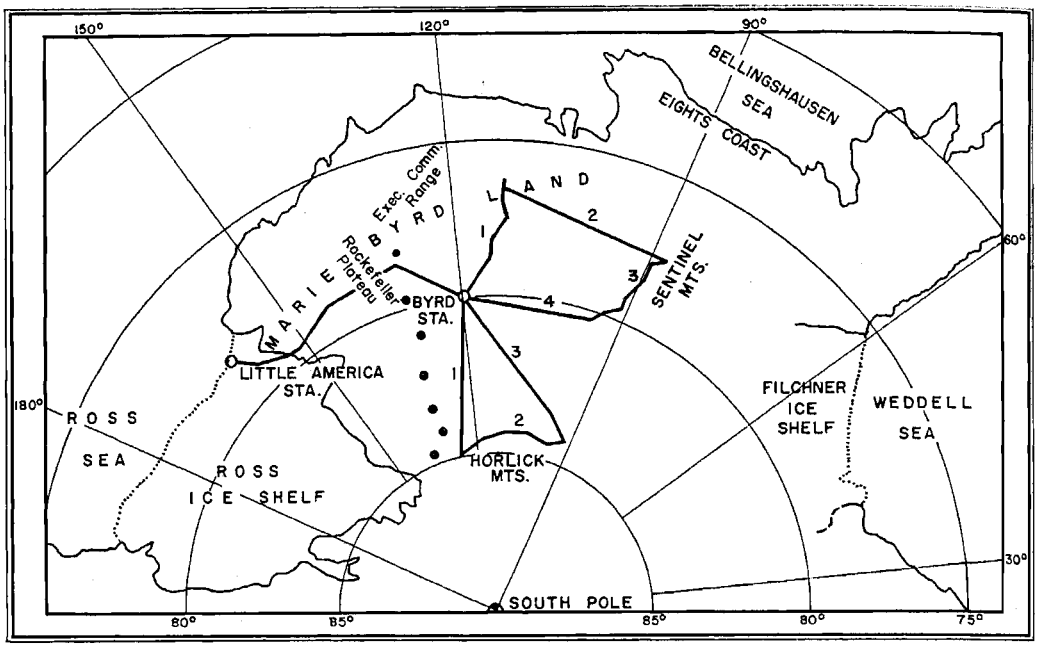

Fig. 8. *Routes of the Three Oversnow Traverses in Marie Byrd Land. The first, in February, 1957, was from Little America Station to Byrd Station. Between November 19, 1957, and February 19, 1958, a four-leg traverse was made in a clockwise direction from Byrd Station to the Sentinel Mountains and back. A third traverse was made from November 1, 1958, to January 20, 1959, taking a counter-clockwise triangular path south of Byrd Station into the Horlick Mountains. Dots are airborne-traverse stations.*

Basal Ice Layer

On a number of reflection records exhibiting a minimum of interference from prolonged surface noise, reflected energy was received several tenths of a second before the main echo from the ice-rock interface. This early reflection was particularly noticeable on records obtained throughout the second leg of the Sentinel Traverse. By combining results of vertical and wide-angle reflections it was possible to determine the existence of a layer at the base of the ice, having a thickness of about 300 meters, in which the primary wave velocity is approximately 3600 m/sec, as compared with 3850 m/sec in the icecap proper.

A comparison of the amplitudes of the early and main reflections shows that the density of the layer must be very close, if not equal, to that of ice. G. de Q. Robin has shown in laboratory experiments that near the melting point the wave velocity in ice decreases very rapidly. It is therefore tentatively concluded that the layer at the base of the icecap consists of ice at the pressure melting point, perhaps either a zone of stagnant ice or a zone of flow. Further study of this layer during future traverses is planned.

Cross-Sections to Bottom

Seismic reflection and gravity results have been combined to draw cross sections of the icecap along the paths shown in Figure 9 for the Little America—Byrd Station Traverse and for the Sentinel Traverse, and, in Figure 10, for the Horlick Traverse. The dashed line in Figure 10 shows an approximate position of sea level relative to the rock surface if the ice were removed and allowance made for "isostatic rebound." (This adjusted position of sea level is here referred to as reduced sea level.)

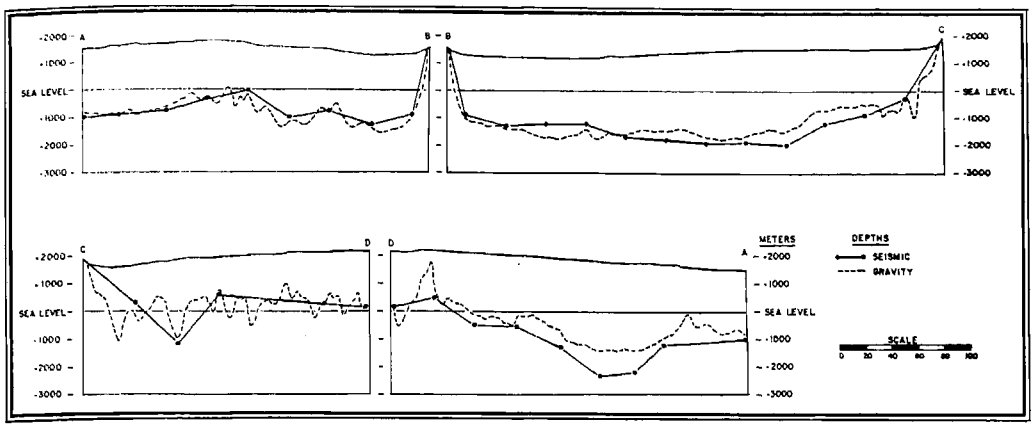

Fig. 9. *Seismic and Gravity Depth Sections Obtained on Byrd-Sentinel Traverses. (Scale in nautical miles.) From the Ross Ice Shelf to the end of the first leg of the Sentinel Traverse, the rock surface is as shown in Section A-B, moderately rough with all but a few peaks well below sea level. The third leg of the Sentinel Traverse, Section C-D, reveals a very rough, mountainous rock surface largely above sea level. The second and fourth legs of this traverse, Sections B-C and D-A, show a deep, smooth, basin-like surface.*

From the Ross Ice Shelf—Rockefeller Plateau boundary to the ends of the first legs of the Sentinel and Horlick Traverses, the picture is generally the same. The rock surface is moderately rough with all but a few peaks well below sea level. The eastern parts of both the Sentinel and Horlick Traverses (leg 3 of the former, leg 2 and the first half of leg 3 of the latter) exhibit a very rough, mountainous rock surface largely above sea level. In intervening areas on the Sentinel Traverse (legs 2 and 4) a deep, smooth, basin-like surface is seen, separated from the mountainous area by a transition zone more or less at reduced sea level.

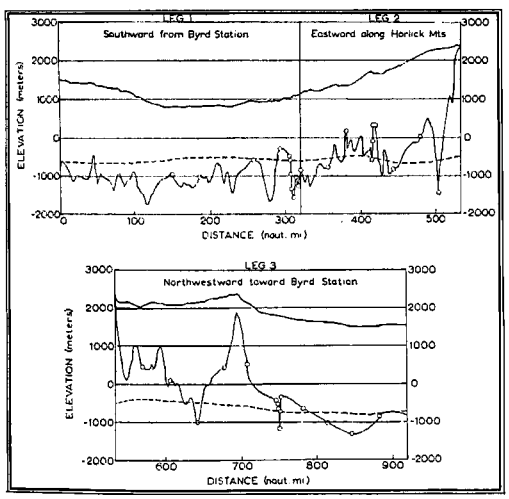

Fig. 10. *Cross Sections of the Icecap and its Underlying Rock Based on Seismic and Gravity Readings Taken on the Horlick Traverse. The dashed line shows sea level as it would be if the ice were removed and allowance made for isostatic rebound.*

Figure 11 is a map of Marie Byrd Land on which are shown contours of the ice surface and a general division into zones depending upon the nature of the rock floor. To the west is an island zone in which the rock level is generally below reduced sea level but with scattered points protruding above. East of this in the northern part of the area is the basin zone, typified by a smooth rock surface beneath the ice. To the west is the high, rugged mountain zone—from the Ross Ice Shelf to the Sentinel Mountains. Between the basin and mountain zones is a transition zone in which the rock surface is more or less flat and at a reduced sea level. The distinction between the island, basin, and transition zones is lost farther south.

The continuity of the mountain zone deserves examination if a decision is to be made on the existence or absence of a trough

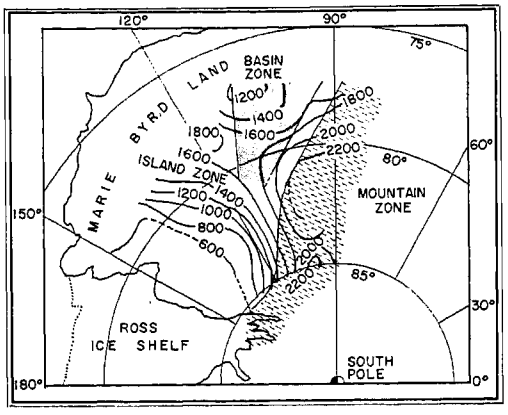

Fig. 11. *Marie Byrd Land Divided into Three Zones According to the Nature of the Rock Floor. In the island zone to the west, rock level is generally below "reduced" sea level, i.e., the adjusted sea level if ice were removed and allowance made for isostatic rebound. To the north is a basin zone, with a smooth rock surface well below reduced sea level. The mountain zone to the east has a high and rugged rock surface beneath the ice. The contours (in meters) show the topography of the ice surface.*

connecting the Ross and Weddell Seas. North of 81°S the Sentinel Mountains and their extension above and below the ice surface form a continuous barrier. In the south, the Horlick Mountains and the subice topography protrude above reduced sea level as far north as 82½°S, with the exception of the narrow deep spot shown on the third leg of the Horlick Traverse at 83½°S.

Thus, it appears that there is no *broad* trough south of 82½°S connecting the Ross and Weddell Seas. Between 81°S and 82½°S there is no north-south coverage far enough east to bear on the problem. More information must therefore be obtained in the vicinity of 90°W before the possibility of a below-sea-level connection can be eliminated.

Ross Sea—Bellingshausen Sea Connection

On the other hand, a connection between the Ross Sea and the Bellingshausen Sea appears likely. Rock surface well below sea level has been found as far north as latitude 77°S, and no known obstacles exist between there and the Eights Coast on the Bellingshausen Sea (Fig. 8). The ice surface exhibits two definite highs, one in the east and the other in the northwest (Fig. 11). Between them is a saddle, indicating flow of the ice from each high toward the other and off to the southwest and north. The profile of leg 1 in Figure 10 shows that the low ice-surface elevations south of Byrd Station are not a reflection of sub-ice topography, and must therefore be attributed to the pattern of ice flow. Thus, the surface contours suggest that there were once two separate ice caps, one centered on the area of the Executive Committee Range and the other along the Sentinel—Horlick axis, and that these two caps converged on the water-covered zone between them.

Geological and magnetic data show the mountains in the two areas to be entirely different in character. Rock samples collected from peaks in the northwest area, as well as the shapes of the peaks themselves, indicate a volcanic origin for these mountains. The magnetic field in this area displays a strong dependence upon rock topography, showing the rock to be of high magnetic susceptibility. In the east, on the other hand, the Sentinels, Horlicks, and intervening nunataks are composed of granite, sediments, and low-grade metamorphic rocks, and do not exhibit strong magnetic character.

Thus, present evidence seems to indicate the division of Marie Byrd Land into two land areas separated by what would be, if the ice were removed, an area of open water running from the Ross to the Bellingshausen Sea.

IGY Bibliographic Notes

This is the twelfth of a series of bibliographic notes on IGY programs and findings. The references are selected largely from an IGY bibliography under preparation in the Science and Technology Division of the Library of Congress.

IGY Bibliography

The first volume of the International Geophysical Year Bibliography is available from the Publishing and Printing Office, National Academy of Sciences, 2101 Constitution Avenue, N. W., Washington 25, D. C. Price $1.00, postage prepaid. The 64-page volume contains 704 references.

The Bibliography is being compiled at the Library of Congress and is a joint project of the Library, the Academy, and the National Science Foundation.

J. Ashbrook, G. F. Schilling, and T. E. Sterne: Glossary of Astronomical Terms for the Description of Satellite Orbits. Smithsonian Contributions to *Astrophysics*. Vol. 2, no. 10. 1958. Pp. 211-214.

D. R. Barber: Origin of Upper-Atmosphere Lithium Atoms Responsible for the New Twilight Airglow at 6708A. *Nature*. Vol. 183. Feb. 7, 1959. P. 384.

Leon Blitzer: Earth Oblateness in Terms of Satellite Orbital Periods. *Science*. Vol. 129. Feb. 6, 1959. Pp. 329–330. Diagr.

C. H. Bosanquet: Change of Inclination of a Satellite Orbit. *Nature*. Vol. 182, no. 4648. Nov. 29, 1958. P. 1533.

S. A. Bowhill: The Faraday-Rotation of a Satellite Radio Signal. *Journal of Atmospheric and Terrestrial Physics*. Vol. 13, nos. 1 and 2. Dec. 1958. Pp. 175–176. Diagr.

K. L. Bowles: Observation of Vertical-Incidence Scatter from the Ionosphere at 41 mc/sec. *Physical Review Letters*. Vol. 1. Dec. 15, 1958. Pp. 454–455. Illus.

R. L. F. Boyd: Space Research. *Nature*. Vol. 183. Feb. 7, 1959. Pp. 361–364.

Chapman, Sydney: The Earth and Its Environment. *Proceedings of the IRE*. Vol. 47. Feb. 1959. Pp. 137–141.

Evert Clark: Pioneer Indicates Restricted Radiation. *Aviation Week*. Vol. 69, no. 16. Oct. 20, 1958. Pp. 30–33. Illus., diagr.

F. F. Evison, C. E. Ingham, and R. H. Orr: Thickness of the Earth's Crust in Antarctica. *Nature*. Vol. 183. Jan. 31, 1959. Pp. 306–308. Diagr., map.

Edwin Flowers: Inside Antarctica No. 2—Amundsen-Scott Station. *Weatherwise*. Vol. 11. Oct. 1958. Pp. 166–171. Illus., map.

O. K. Garriott and O. G. Villard, Jr.: Antipodal Reception of Sputnik III. *Proceedings of the IRE*. Vol. 46, no. 12. Dec. 1958. P. 1950. Illus.

M. J. Hendrie: The Photographic Observation of Artificial Satellites. *Spaceflight*. Vol. 1, no. 8. July 1958. Pp. 267–274. Illus., diagr.

H. A. Hess: Registrierung des Sputnik II Auf 40.002 KHZ. *NTZ*. Vol. 11, no. 7. July 1958. Pp. 347–348. Illus., diagr.

N. E. Howard: *Handbook for Observing the Satellites*. New York, Thomas Y. Crowell, 1958. P. 136. Illus., diagr., maps.

International Geophysical Year. *WMO Bulletin*. Vol. 7. Oct. 1958. Pp. 154–156. Illus.

V. A. Kotel'nikov, V. M. Dubrovin, V. A. Morozov, O. N. Rzhiga, and A. M. Shakhovskoi: Determination of Satellite Orbit Parameters With the Use of the Doppler Effect. *Physics Express*. Vol. 1, no. 3. Sept. 1958. P. 33.

IGY Special Studies in Meterology. *Weatherwise*. Vol. 12, no. 2. April 1959. Pp. 67–72. Diagr., maps.

Jacchia, Luigia G.: Two Atmospheric Effects in the Orbital Acceleration of Artificial Satellites. *Nature*. Vol. 183. Feb. 21, 1959. Pp. 526–527. Diagr.

Krassovsky, V. I.: Exploration of the Upper Atmosphere with the Help of the Third Soviet Sputnik. *Proceedings of the IRE*. Vol. 47. Feb. 1959. Pp. 289–296. Illus., diagr.

Marshall Melin: Man's Farthest Step into Space. *Sky and Telescope*. Special Supplement. Vol. 18, no. 1. Nov. 1958. Pp. 1–8. Illus., diagr.

R. H. Merson, D. G. King-Hele, and R. N. A. Plimmer: Changes in the Inclination of Satellite Orbits to the Equator. *Nature*. Vol. 183. Jan. 24, 1959. Pp. 239–240. Diagr.

W. B. Moreland: Inside Antarctica No. 3—The Weather Central at Little America. *Weatherwise*. Vol. 11. Dec. 1958. Pp. 196–200. Illus., maps.

Robert R. Newton: Lifetime of Artificial Satellites. *Jet Propulsion*. Vol. 28, no. 5. May 1958. Pp. 331–333.

Nicolet, Marcel: The Constitution and Composition of the Upper Atmosphere. *Proceedings of the IRE*. Vol. 47. Feb. 1959. Pp. 142–147.

Yngve Öhman: Solar Flares and Surges Observed at the Swedish Astrophysical Station in Anacapri in the Year 1957. *Stockholm Observatoriums Annaler*. Vol. 20, no. 7. 1958. Pp. 1–38. Illus., diagr.

Glauco Partel: Il "Pioneer" Primo Concerto Tentativo Verso la Luna. *Rivista Aeronautica*. Vol. 34, no. 11. Nov. 1958. Pp. 1649–1656. Illus.

Routledge, N. A.: Russian Contributions to the International Geophysical Year. *Nature*. Vol. 183, No. 4668. April 18, 1959. Pp. 1087–1088.

G. F. Schilling and T. E. Sterne: Densities and

Temperatures of the Upper Atmosphere Inferred from Satellite Observations. *Journal of Geophysical Research.* Vol. 64. Jan. 1959. Pp. 1-4. Diagr.

C. A. Schroeder, E. J. Habib, and W. R. Silvester: Time Standard. *Naval Research Laboratory Report No. 5227.* Oct. 22, 1958. P. 44. Illus., diagr. (Project Vanguard Report No. 36; Minitrack Report No. 8; PB Report No. 151169).

T. J. Seed: V.H.F. Observations on the Aurora Australis. *Journal of Geophysical Research.* Vol. 63. Sept. 1958. Pp. 517–526. Illus., diagr.

Yoshida Sekiko and Masami Wada: Storm-Time Increase of Cosmic-Ray Intensity. *Nature.* Vol. 183. Feb. 7, 1959. Pp. 381–383. Diagr.

R. L. Smith-Rose: Electron Density Profiles in the Ionosphere During the IGY. *Journal of Geophysical Research.* Vol. 63. Sept. 1958. Pp. 570–572.

Strahlungsmessungen Durch Explorer IV: *Raketentechnik und Raumfahrtforschung.* Vol. 2, no. 4. Oct. 1958. Pp. 131–132. Diagr.

Swedish-Finnish-Swiss International Year Expedition to Nordaustlandet, 1957–58, and Swedish Expedition to Nordaustlandet, 1958–59. Season 1957–58. *Polar Record.* Vol. 9. Jan. 1959. Pp. 338–339.

M. C. Thompson, Jr., and D. M. Waters: Comparison of Phase Difference and Doppler Shift Measurements for Studying Ionospheric Fine Structure Using Earth Satellites. *Proceedings of the IRE.* Vol. 46, no. 12. Dec. 1958. P. 1960. Diagr.

Unwin, R. S.: The Geometry of Auroral Ionization. *Journal of Geophysical Research.* Vol. 63. Sept. 1958. Pp. 501–506. Illus., diagr.

Venkiteshwaran, S. P.: Atmospheric Electricity Observations in India during the IGY—Radiosonde Techniques for Measuring Potential Gradient and Conductivity. *Journal of Scientific and Industrial Research.* Vol. 17A, no. 12. Dec. 1958. Pp. 24–32. Illus., diagr.

E. Woyk (E. Chvojková): Investigations of the Ionosphere Using Signals from the Earth Satellites. *Nature.* Vol. 182, no. 4646. Nov. 15, 1958. Pp. 1362–1363. Diagr.

Vol. 40, No. 3 TRANSACTIONS, AMERICAN GEOPHYSICAL UNION September 1959

NATIONAL ACADEMY OF SCIENCES

Number 26 • August 1959

IGY BULLETIN

A monthly survey of programs and findings of the International Geophysical Year and the International Geophysical Cooperation-1959 as related primarily to United States programs.

Unusual Radio-Signal Enhancement in the Far East

The following report is based on material supplied by J. W. Finney, E. K. Smith, L. H. Tveten, and J. M. Watts, of the Central Radio Propagation Laboratory, National Bureau of Standards' Boulder Laboratories, and Ross Bateman, of Page Communications Engineers, Inc. A more detailed account was published in the Journal of Geophysical Research, *April 1959.*

Radio propagation studies in the eastern Pacific just prior to and during the IGY revealed an anomalous increase in the intensity of very-high-frequency (VHF) radio signals over several propagation paths between the Philippines and Okinawa. The enhancement occurred during the evening, beginning about two hours after sunset and lasting until about midnight. It was particularly strong during the autumnal equinox.

Signals with frequencies above about 30 megacycles per second are not generally reflected by the ionosphere, but penetrate it completely and continue into space. Under certain special conditions, however, generally by "scatter" and by "sporadic-E" propagation, ionospheric transmission may be effected at frequencies up to about 100 mc/sec. Scattering results from irregularity of surfaces of equal ionization density in the ionosphere or from discontinuity of the electron density at some level; generally, such turbulent conditions result in partial reflection of the original wave energy up to frequencies considerably higher than normal. Sporadic E is probably the result of reflections from clouds or patches of unusually high ionization in the E region of the ionosphere.

Propagation of VHF radio signals along paths between the Philippines and Okinawa normally takes place by scatter in the lower ionosphere or, occasionally, by sporadic E. The IGY equipment that monitored the enhanced signals was originally set up by the Central Radio Propagation Laboratory (CRPL) to measure sporadic-E propagation. However, the abnormal signal enhancement observed along these paths was often as much as 30–40 decibels above normal at a frequency of about 50 mc/sec, and 40–50 db above normal at about 36 mc/sec.

The experiments described were made with the cooperation of the Voice of America, the US Army IGY Support Group, and the Philippine IGY Committee.

Observational Circuits

The anomalous enhancement was first measured over an experimental circuit at 36.4 mc/sec between Poro Point, Philippine Islands, and Sobe, Okinawa (1329 kilometers), operated from May 1956 to

May 1957. The IGY circuit designed to measure sporadic E began operating in September 1957 at 49.84 mc/sec over a nearly identical, 1347-kilometer circuit between Poro Point, P. I., and Onna, Okinawa.

During the May 1956–1957 period of operation at 36.4 mc/sec, peaks in the number of occurrences of the evening enhancement were reached during both the spring and fall equinoctial periods. In the following year, however, at 49.84 mc/sec, only the fall peak was observed; during the 1957 spring equinox, in fact, there appeared to be a minimum in the number of occurrences.

Figure 1 is a graph showing monthly medians of hourly median signal intensities for both propagation paths during the months of October and November 1956 and 1957. It can be seen that in both years October was a month in which the anomaly occurred very often and November was a month of few occurrences.

Based on the observations at 50 mc/sec and below, it has been estimated that the intensity of the anomalous signal decreases by about one decibel for each megacycle of frequency increase. If this estimate is also valid for frequencies above 50 mc/sec, it may be possible to distinguish the unusual enhancement to frequencies as high as 80–90 mc/sec.

An additional propagation path was set up between Okinawa and the Manila area to observe the behavior of the anomaly. Southbound transmissions were at 36.4 mc/sec. At each terminal, dipole antennas were

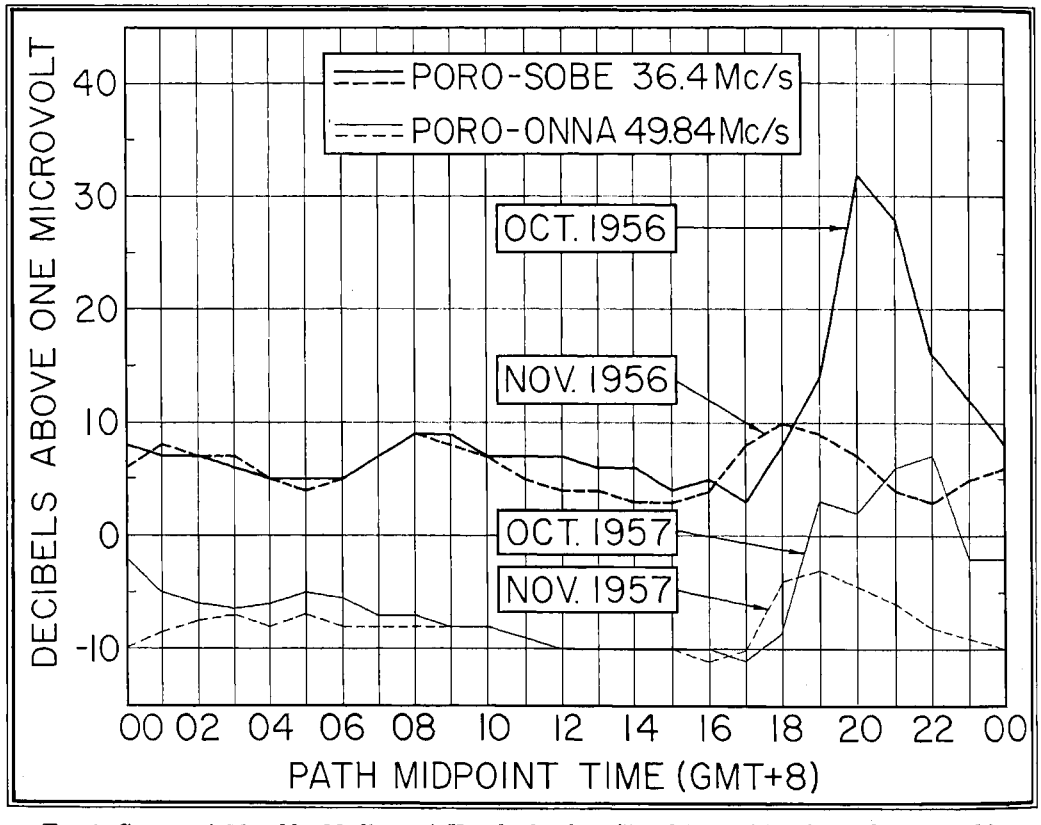

FIG. 1. *Curves of Monthly Medians of Hourly Median Signal Intensities Over the Two Philippines-Okinawa Propagation Paths. The evening-hour intensity increase is clearly shown, as well as the tendency for the enhancement to occur frequently in October and relatively infrequently in November.*

alternated at half-hour intervals with corner-reflector antennas. For the northbound transmissions, at 40.2 mc/sec, antennas beamed on the great-circle path between the two points were alternated at half-hour intervals with symmetrical split-beam antennas at each end. The split-beam antennas had a radiation pattern with beam maxima about 8° on each side of the great-circle path, and a "null" along the great-circle path itself.

It appears that most of the time during periods of abnormally enhanced propagation, the signals arrive from directions predominantly on one side or the other of the great-circle bearing. Occasionally, and particularly during the later stages of the periods of enhancement, extremely strong signals were received along the great-circle path. During these times, the intensity of signals observed with the split-beam antennas was characteristically lower than the intensity of signals received with the "normal" beam.

Pulse Experiments

Pulse measurements were made over the Poro Point-Onna path in September 1958. In such experiments, short, pulsed signals are sent into the ionosphere and the time between transmission and reception is measured. Assuming that radio signals travel at the speed of light, the height of the reflecting layer can then be computed.

For the pulse experiment, a peak pulse power of two kilowatts was used and independent time standards were employed to control the pulse repetition rate (100/sec) at the transmitter and the oscilloscope sweep rate at the receiver. Records were obtained for four nights. The normal E-region echo was shown at the bottom of each record so that the time delay of the abnormal echo could be compared to it.

The records for both September 22 and 23, 1958, show an abrupt start of the anomalous signal at a time delay of about 1200 microseconds behind the E-region pulse. The commencement time for the anomalous signal was 1924 (local time) on September 22 and 1911 on September 23. On the 22nd, the delay time had decreased to 500 microseconds by 2300 and on the 23rd it fell to 600 at 2130, after which the E-region echo dropped out entirely.

A delay of 400 microseconds relative to the E-region echo corresponds geometrically to a reflection height of about 300 kilometers at the mid-point of the great-circle path; a delay of 1100 microseconds corresponds to a height of about 500 kilometers. Small lateral deviations from the great-circle path would not materially affect these figures. The transmitted pulse —50 microseconds long—was broadened to approximately 1500 microseconds in the earlier hours; this value decreased to less than 500 microseconds in the later stages of the enhanced propagation.

Comparisons with Other Stations

The periods of anomalous propagation over the Poro Point-to-Onna path during September 1957 were compared with ionospheric data from the ionosphere stations at Baguio, P. I., and on Okinawa. No association could be found between the anomaly and E-region effects. The abnormal propagation periods did, however, appear to correspond to periods of spread-F propagation at Baguio and of high F2 critical frequencies at Okinawa, where spread F is comparatively rare. (Spread echoes are scattered through a frequency range of several megacycles instead of remaining at the transmission frequency. Spread-F scattering occurs in the F region of the ionosphere. Critical frequencies are the maximum frequencies reflected by the individual ionospheric layers. Critical frequencies vary with ionosphere conditions.)

Values of the F2 critical frequency observed at the Okinawa ionosphere station in the evening hours are among the highest

in the world. The F2 maximum usable frequency (MUF) for the Poro Point-Onna propagation path is often as high as 35 mc/sec, and may have reached 40 mc/sec on at least one occasion. It might be argued, therefore, that the unusually intense propagation in the 35–40 mc/sec range derives from some peculiarity related to the F2 critical frequency. However, the fact that this anomaly has also been observed at approximately 50 mc/sec makes this hypothesis untenable.

Recent measurements during the enhancement indicate a fading rate on the order of 5 cycles/sec at a frequency of 50 mc/sec. This is approximately the same as the fading rate for normal scatter fading; the fading rate for periods of sporadic-E transmission, however, is usually much lower.

There is some evidence of a small negative correlation with magnetic activity. At the mid-points of the Philippines-to-Okinawa propagation paths, the magnetic dip of the ionosphere is about 28°. A circuit from Panama to Guayaquil, Ecuador, operated at 50 mc/sec by the National Bureau of Standards in the latter part of the IGY, although having roughly the same magnetic configuration as the Philipines-Okinawa paths, has shown few occurrences of the abnormal signal enhancement. Some observations of what appears to be the same anomaly have been made on winter nights at 50 mc/sec over a path between Panama and the US Naval Base at Guantanamo Bay, Cuba. This path has a magnetic inclination of 44° at mid-point.

Conclusions

The investigators believe that results of the experiments described indicate that the anomalously intense signal is propagated via the F region of the ionosphere and is associated with low-latitude spread F, as observed with ionosphere sounders. The relatively well-defined lower edge of the anomalous echo (usually present in visual records of scattered signals) can be interpreted in either of two ways: (1) It may represent the limiting geometric distance to the lowest stratum of ionized "blobs" in the F region; or (2) it may be the closest approach of the locus of the specular, or reflecting, condition in the F region that permits optimum scattering from blobs of ionization aligned parallel with the earth's magnetic field. The investigators consider the latter interpretation more probable.

Aurora Observations at the South Pole

This report is based on material prepared by C. W. Gartlein, B. Nack, and G. Sprague of the IGY Visual Auroral Data Center, Cornell University.

Three main conclusions have been drawn from aurora observations at the South Pole and other US-IGY Antarctic stations. They concern the location of the auroral zone; the daily shift of the position of the zone, and the effects of twilight on auroral reporting.

The results of visual auroral observations at US-IGY South Pole Station have a special interest because of the relatively fixed relation between the observers and the sun. In particular, the sun maintains an almost constant depression below the horizon for forty days starting at the first of June. Hence, auroral observations for

this time and place are not complicated by the effect of twilight on visibility.

Auroral Distribution

The South Pole observations show that, within the region circled by the zone of maximum auroral frequency (see Fig. 2), there is a definite increase in the number of overhead auroras with distance from the geomagnetic pole. Taking into account similar data from other US-IGY stations, it appears that the southern region of maximum aurora frequency is outside (north of) NAF McMurdo and Little America, Byrd, Wilkes, and the South Pole Stations, but inside Ellsworth Station.

Based on South Pole and other auroral observations, together with theoretical calculations based on the earth's magnetic field, the authors have determined the approximate positions of three major boundaries of auroral activity. These boundaries are shown in Fig. 2.

Line A represents the outermost edge of the biggest auroras seen during the IGY. This boundary passes between the two main islands of New Zealand.

Line B is the outermost edge of the region in which the greatest number of au-

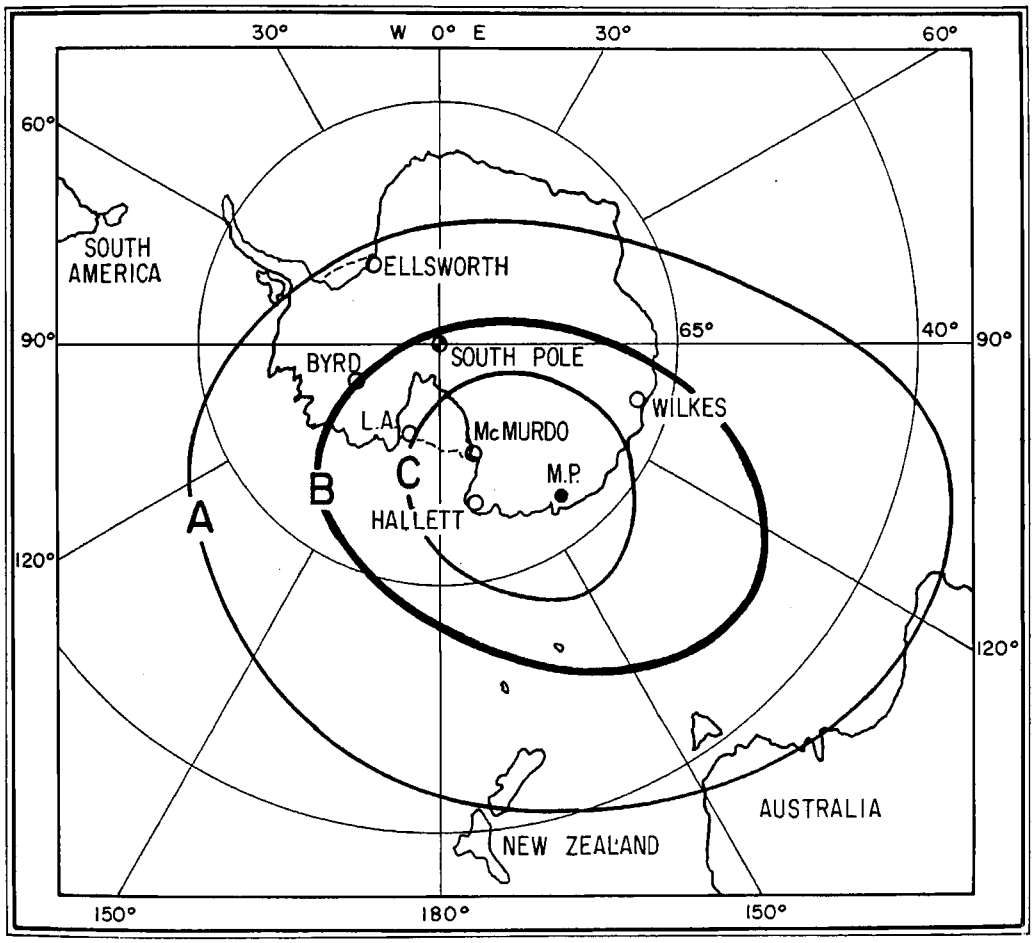

FIG. 2. *Aurora Australis. Line A represents the outermost edge of the biggest auroras seen from the South Pole and other stations during the IGY. Line B is the outer edge of the region where the greatest number of auroras are seen. Line C bounds a zone inside which "irregular" auroras occur. LA identifies Little America Station, MP the magnetic pole.*

roras are seen, and therefore is an approximation of the southern auroral zone.

Auroras occurring inside C are somewhat different from those reported outside C in that arc forms and flames are not seen. Instead, the display consists of rays and surfaces; both are distributed in patches and the small individual features are of short duration, giving a flickering appearance rather than regular pulsations.

Daily Motion

A noteworthy feature of the auroral distribution is a shift in the latitude of most frequent occurrence during the day. At about 01 hours UT, the South Pole observers noted auroras most frequently in the part of the sky toward Ellsworth Station. Near 17 and 18 hours UT, however, the concentration had shifted to the opposite part of the sky, or toward the geomagnetic pole. (See *Bulletin No. 12* for method of calculating ground point over which aurora occurs.)

TABLE 1
Frequency of Auroras Seen by South Pole Observers, 6/1/57–7/14/57, By Hour and Latitude

°S Lat.	86	87	88	89	90	89	88	87→(GMP)
UT								
00	15	18	15	5	7	12	15	
01	9	9	9	4	3	12	15	50
02	12	3		3	4			
03	9	6		2	5			
04	3				1			
05		6		2	1			
06	6		3	1	1			
07		3	6					
08	3	3	6	2	2			
09			3	2				
10	6		6	4	3			
11	3	12	3	2	5			
12	3			1	7			
13		9		5	6		15	
14			3	3	1	4		
15			3	1	3	12		
16				3	3	4		
17				1	3			
18		6	6	1	1	8	15	
19	3	9	12	7	4	12		
20	12	6	12	8	9	12	15	
21	3		9	5	5	12		50
22	12	18	6	6	6	8	15	
23	6	6	3	4	6	12	15	

Note: The unit used is the number of forms reported divided by the number of clear observation hours.

Table 1 indicates the frequency of auroras seen by South Pole observers at different hours of the day in different parts of the sky along their geomagnetic meridian (i.e., the meridian from the geomagnetic pole that passes through the zenith point above the station). The parts of the sky are identified in term of degrees of geographic latitude along this geomagnetic meridian. The tabulation starts at the left, from the part of the sky toward Ellsworth Station. The columns to the right show frequency of auroral observations in parts of the sky southward along the geomagnetic meridian to the geographic pole, then northward toward the geomagnetic pole. The individual numbers represent the percentage of auroral sightings in a given region in a given hour.

When averaged over three-hour periods, the general trend is toward more frequent auroral observations in the part of the sky toward the geomagnetic pole as the UT day progresses. It is reversed after 17 or 18 hours UT.

This daily effect completely obscures any effect sunlit auroras might have on the frequency of auroral observations. (Sunlit auroras occur at heights above that of the earth's shadow.) The sunlit auroras should increase observations at 4 to 6 hours UT in that part of the sky nearer the sun, i.e., in the direction toward the geomagnetic pole. In fact, however, Table 1 records no auroras during these hours in this part of the sky. Instead, the maximum occurs in the opposite direction. Similarly, when the South Pole is between the sun and the magnetic pole, at about 16 hours UT, the majority of auroras are seen to occur in the direction opposite to the sun.

The daily effect is probably due to the apparent motion of the earth's magnetic

field with respect to the South Pole and the sun. This implies a seasonal effect.

Twilight Effect

The aurora sightings per hour are fairly constant until the sun climbs to a point about 18° below the South Pole's horizon. Then, sightings decline with the sun's continued rise toward the horizon. This twilight effect is probably physiological, i.e., the observers become unable to distinguish faint auroras against a brighter sky, rather than a physical effect in which sunlight in some way desensitizes the atmosphere to auroras. It is, therefore, advisable to treat with reserve data obtained when the solar angle of depression is less than 18°.

Second Brown Bear Cruise

The following material is based on a report submitted by Richard H. Fleming and staff, Department of Oceanography, University of Washington. An earlier IGY cruise of the Brown Bear *is described in* Bulletin No. 9.

During the summer of 1958, the oceanographic research vessel *Brown Bear*, of the University of Washington, carried out its second IGY cruise (*Brown Bear* Cruise 199). The ship left Seattle, Washington, on June 30, 1958, and returned on August 20. The cruise track covered an area of the Pacific generally west of the United States, reaching as far as 146°40′W, as far south as approximately 32°N, and including stops at San Diego and San Francisco, California (see Fig. 3).

The major objectives of the cruise were (a) to reoccupy hydrographic stations originally occupied by the research vessel *Carnegie*, in 1929, to determine what changes may have occurred in the properties of the deep water during the 29-year interval, and (b) to study the transition zone between Sub-Arctic and Sub-Tropic Water masses in the Northeast Pacific. In addition, a comprehensive program of oceanographic sampling was carried out along the cruise track.

This report outlines the observation program on the cruise and gives some of the preliminary results. It appears from these preliminary analyses that the warmer subtropical waters moved farther north than usual in the eastern Pacific during the summer of 1958.

Chief Scientist for the cruise was Maurice Rattray, Jr.; the *Brown Bear* was under the command of Captain F. W. Princehouse.

Observation Program

Routine observations were made at 42 hydrographic stations during the second IGY cruise of the *Brown Bear*. Three of these stations were inshore, contiguous to Puget Sound. In addition, a mid-water trawl was used to collect specimens for marine biology studies, and a program of albacore tagging was undertaken by R. L. Ridenhour, biologist, Oregon State Fish Commission.

Routine chemical analyses of sea water were carried out. The suspended matter filtered out of some samples will be subjected to spectrographic analyses to determine inorganic composition and distribution of trace elements (elements other than the eight relatively abundant rock-formers —O, Si, Al, Fe, Ca, Na, K, and Mg).

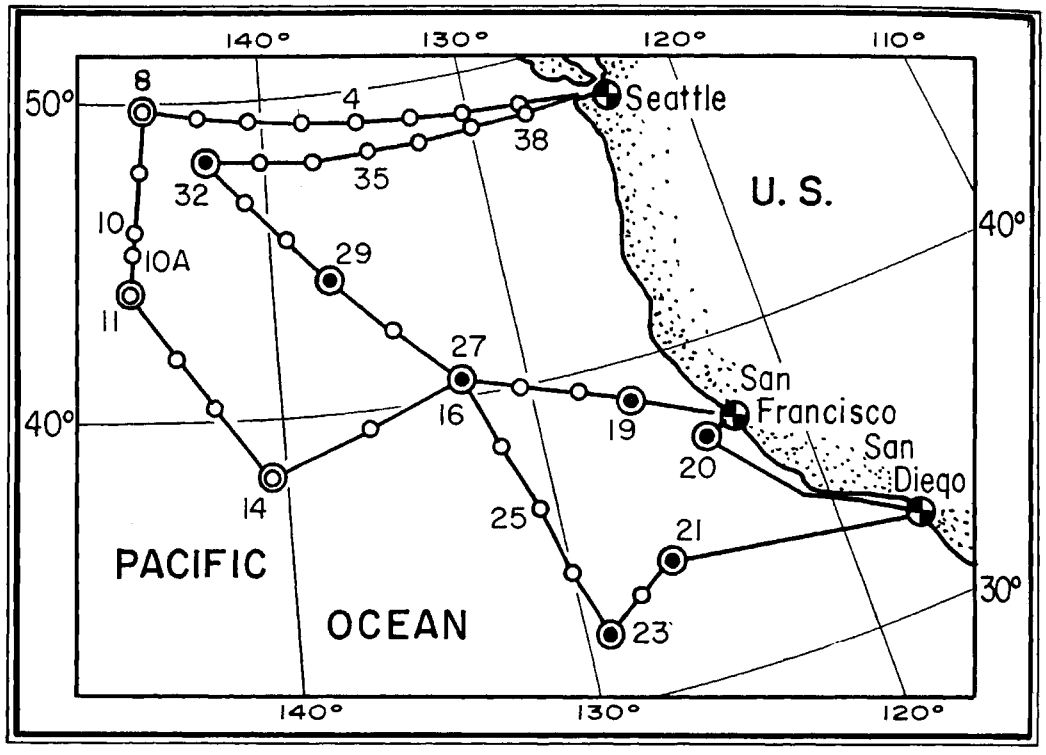

FIG. 3. *Track of Second IGY Cruise of* Brown Bear. *Single small circles represent standard hydrographic stations: double circles represent deep stations, with black dots signifying those previously occupied by the research vessel* Carnegie *(1929).*

Water samples for C-14 analysis were obtained from a depth of 100 meters above the bottom at 11 stations and from the minimum oxygen layer at 5 stations. (Some oceanographers believe that oxygen distribution in the ocean is closely related to water motion, and that layers of minimum oxygen content represent layers of minimum horizontal movement.)

Bottom cores were obtained along the cruise track to determine carbonate distribution and the magnesium-to-calcium ratio in carbonate bottom sediments.

Temperature-salinity curves and vertical sections of density were compiled for each hydrographic station occupied. Geopotential topographies of various pressure levels were also compiled. (Geopotential topography is determined by computing the varying values of density at any given depth. The horizontal hydrostatic pressure gradient determined from the density variation balances the Coriolis force—the effect of the earth's rotation on moving bodies; hence, study of geopotential topography supplies information on the strength and direction of currents. The pressure of the water is described in terms of decibars—1 decibar [10^5 dynes/cm^2] represents very nearly the force exerted by a column of water 1 meter high.)

Physical Oceanography

Brown Bear Cruise 199 covered the eastern portion of the transition zone between the Sub-Arctic and Central Water masses, including the region where the Sub-Arctic Current splits into the Alaska and California Currents.

(Sub-Arctic Water is cold, with temperatures of 35°–39°F, and has low salinity at

the surface. North of about 45°N it flows generally eastward, part of it turning north as it approaches the West Coast of the US and part turning south at the coast to mix with Equatorial Water in the vicinity of 25° N. The Central Water is warmer and more saline than Sub-Arctic Water, and may originate approximately within the region 30°–40°N, 150°–160°E. Intermediate Water generally occurs below Central Water in the vicinity of 36°N and is characterized by a salinity minimum layer. Equatorial Water occurs mostly south of about 15°N and is warmer and generally more saline than the other water masses.)

Water Masses: Temperature-salinity diagrams for the Northeast Pacific during the summer of 1958 indicate that the distribution of water-mass types was generally similar to that reported by Canadian oceanographers for the summers of 1955-57, although warmer waters apparently moved farther north than usual.

In summer 1958, Sub-Arctic Water was centered along 45°N, entering the cruise area from the west as a band about 100 miles wide and increasing in width toward the east. At 130°W, this band of water stretched almost from 40° to 50°N (a width of nearly 600 miles), and evidently marked the boundary region where the eastward-flowing Sub-Arctic Current splits northward into the Alaska Current and southward into the California Current. Since the contours of geopotential topography spread apart (indicating weak pressure gradients) as they approached the coast (see Figs. 4 and 5), it appears that this wide band of Sub-Arctic Water had accumulated in a large area of weak currents off the coast.

Water below the halocline (zone of rapid increase of salinity, just beneath the surface layer) consisted of mixtures of Sub-Arctic Water with (a) Intermediate Water, (b) Central Water, or (c) Equatorial Water.

In the southeastern half of the cruise area, an appreciable amount of Equatorial Water was mixed with the Sub-Arctic Water at depths greater than 1100–1900 feet (depending upon location).

Between these levels and the halocline, the water consisted of a mixture of Sub-Arctic and Intermediate Waters. Intermediate Water made up a large proportion of the mixture generally in the southwestern part of the cruise area, and there seemed to be appreciable amounts in the central, east-central, and northeast part of the area. In the extreme southern and southwestern part of the cruise area, some Central Water could be found between the bottom of the halocline and the top of Intermediate Water layer.

Geopotential Topography: South of 50°N and west of 135°W, the geopotential topography of the surface relative to the 1200-decibar level (see Fig. 4) indicated a northeasterly flow of Sub-Arctic Water; east of 130°W, southeasterly flow is indicated in these latitudes. Water crossing the 50°N parallel in the region west of 130°W apparently continued northward into the Gulf of Alaska.

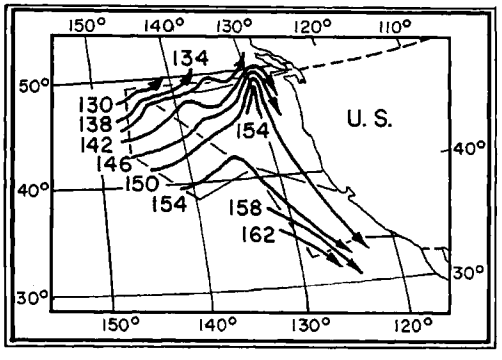

FIG. 4. *Geopotential Topography of the Sea Surface Relative to the 1200-decibar Level in the Cruise Area. Arrows show direction of current flow; contours are numbered in dynamic centimeters. (A dynamic centimeter represents the amount of work required to move a given mass through a vertical distance of one centimeter).*

The surface geopotential topography varies considerably from year to year in this region. The most notable features for 1958, compared to the previous three summers, were the existence of a northward component of flows over the whole western part of the area and concentration of the contours (indicating greater velocities) near 49°N, the highest such concentration during the period 1955–58.

The geopotential topography of the 200-decibar level relative to the 1200-decibar level had the same general features as that of the sea surface (see Fig. 5), but with

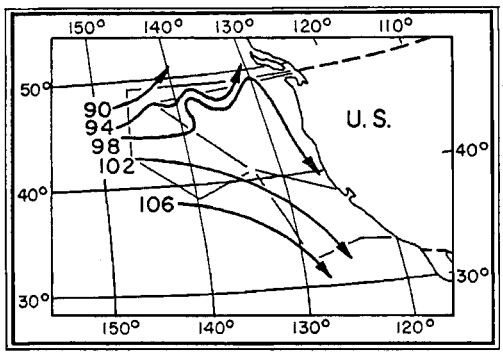

FIG. 5. *Geopotential Topography of the 200-decibar Surface Relative to the 1200-decibar Level. Arrows show direction of current flow; contours are numbered in dynamic centimeters.*

decreased velocities. The primary difference was that currents south of 45°N everywhere tended toward the south rather than toward the north, as they did at the surface west of 130°W.

Current Velocities: Throughout the cruise area, average currents were weak—about one mile per day—although locally currents at times reached 4–7 miles per day. The highest velocities were present near the coast of Washington State between 48°N and 50°N, where a portion of the northeast-flowing Sub-Arctic Current turns southeast along the coast. A region of rather weak currents, centered at about 45°N, 130°W, corresponded to a pressure ridge around which this stronger current flowed.

At the 200-decibar level, the strongest currents lay along a line from about 45°N, 146°W, to 49°N, 130°W, defining the front between the Sub-Arctic and Intermediate Water masses. Vertical sections of density verify the position of this front.

Temperatures: Unusually high surface temperatures and deeper-than-average thermoclines were evident in 1958. (The thermocline is a layer in which temperature decreases rapidly with depth.) The lowest surface temperature, 53.5°F, was measured in the northwest corner of the cruise area, with temperatures increasing toward the south and the east. The maximum temperature, 68.9°F, was observed at approximately 39°N, just north of Station 26 (Fig. 1).

The warmer-than-usual surface temperatures lay roughly in the region south of the subsurface front marking the transition between Sub-Arctic and Intermediate Waters and north of a surface front, 165–330 feet deep, at about 40°N near Station 13. This surface front also gave a southern limit to the currents turning northward along 130°W.

The vertical temperature structure was generally characterized by (a) a relatively uniform upper layer, (b) a thermocline layer, and (c) a layer in which the temperature gradient was small and decreased with depth. The maximum temperature gradient was generally near the top of the thermocline, at a depth of about 100 feet. Offshore, the thermocline appears to have been deeper in 1958 than the average for the period 1941-52; farther west it became shallower.

Rough estimates of the rate of change of surface temperatures were made in different parts of the cruise track on both outbound and return legs. They were as follows:

Areas	*°F/month*
Stations 16, 27	6.0
" 7, 8, 9, 32	1.6
" 1, 38	1.3

Conclusions: Departures from normal in this region during 1958 seemed to result from differences in surface flow, which in turn strongly suggests that these departures were caused ultimately by differences in the related wind systems. There is also evidence, however, that the flow in this region is inherently unstable, in which case the 1958 conditions may represent a northward "meander" of the water masses.

Marine Biology

Midwater Trawling: Over 300 trawls were made, with 3 to 8 samples taken almost every night. Daylight trawls were also made for comparison. The distribution of marine fauna reflected the higher than average temperatures and the transitions from one water mass to another.

Preliminary examination of the trawl samples revealed the following:

(a) Catches close to the coast, particularly in the northern part of the cruise area, were surprisingly small compared with those obtained during the first IGY cruise of the *Brown Bear*. These small catches appear to be related to the relatively high temperature of the inshore waters, which suggests a tongue of water encroaching from the south. West of about 133°W, catches approximated those of the earlier cruise. The largest catches were made in the northwest corner of the area.

(b) In the northern areas, a pronounced thermocline seemed to act as a barrier to the plankton. (Plankton—floating or weakly swimming animal and plant life—is a basic food resource for other marine life.) Catches were extremely small in hauls made above the thermocline. In the single exception, a large catch taken in a shallow haul between stations 37 and 38, most of the animals appeared typically southern. The peak abundance occurred below the thermocline, at a depth of 200 feet; these catches were typically northern.

(c) A definite change in the character of the marine life occurred between stations 9 and 11, corresponding to the transition zone between Sub-Arctic and Intermediate Water. Hauls taken between stations 9 and 10 showed typically northern populations, whereas hauls just south of station 10 were lower in plankton volume and more typically southern. At least eight fish species not captured to the north were taken south of station 10; large catches of hatchet fish, *Argyropelecus spp.*, were particularly unusual. On the return leg of the cruise, the faunal split occurred between stations 30 and 32.

(d) Plankton catches with the midwater trawl were very small south of 37°N, except in hauls made close to the California coast. The offshore catches were approximately 1/100 the volume of hauls made to the north at similar longitudes.

(e) An extensive temperature inversion layer at 400–500 feet, first noticed south of station 10A, was probed with the midwater trawl and followed south to station 14. Catches above and below the inversion were small, but within the inversion they were large, approximating catches normally expected closer to the surface in northern waters. Although plankton catches decreased in volume to the south, the peak catches were always made within the inversion layer.

(f) Numerous bathypelagic (deep-sea) fishes were captured during the cruise. The largest fish caught was a 4-foot specimen of the king of the salmon, *Trachypterus rex-salmonorum;* several larvae and juveniles of this fish were also taken.

Albacore Tagging: Albacore were trolled for and tagged between Seattle and San Diego. From June 30 to July 23, a total of 38 albacore was caught, of which 29 were

tagged. This species of tuna, 15–30 inches long and weighing 4–30 pounds, is commonly found in temperate and tropical waters. Tagging supplies information on migration patterns, population composition, and sometimes on growth patterns of the fish.

A large concentration of albacore was found at approximately 46°N, 146°30′W, on July 11. Surface-water temperatures were 57° to 58°F; analysis for possible relationships with other local oceanographic conditions must await further processing of the available data. Other catches were sporadic and indicated no appreciable concentrations of albacore.

Stomach analyses of the untagged fish indicated that sauries (narrow-bodied, spiny-finned fish with widely-forked tails) were their principal food, with pelagic shrimp, squid, and amphipods (crustaceans resembling sand fleas) also noted.

Antarctic Notes

Continental Structure

New Zealand scientists, interpreting seismic records obtained during the IGY at Scott Base (NZ) and Hallett Station (NZ-US), report the existence of continent-type crustal structure beneath the ice mantle of a large portion of East Antarctica. The report, by F. F. Evison, C. E. Ingham, and R. H. Orr, of the New Zealand Department of Scientific and Industrial Research, appeared in *Nature,* January 31, 1959.

Records of the dispersion of seismic waves traveling through the crustal rocks from their point of origin, the epicenter of an earthquake in the southeast Indian Ocean on September 9, 1957, were analyzed. They showed the earth's crust to be approximately 35 kilometers thick in the region from the Wilkes Coast east of US-IGY Wilkes Station to the Ross Sea area, a distance of about 2000 km. (Preliminary analyses for an earthquake that occurred in the southwest Indian Ocean on August 4, 1957, also show a crustal thickness of about 35 kilometers for East Antarctica.) The normal thickness beneath continents ranges from about 30 to 40 kilometers. "Thus," the report states, "the existence of a true Antarctic continent is confirmed."

In the US program, analyses of dispersion of surface seismic waves from earthquakes in oceanic areas adjacent to the US-IGY Wilkes Station also suggest continental structure in this part of the Antarctic. These analyses indicate an average crustal thickness of about three-fourths the value considered normal for continents. On the basis of data gathered throughout the Antarctic during the IGY, G. P. Woollard, member of the USNC-IGY Technical Panel on Seismology and Gravity, has stated: "After even a crude calculation . . . it appears that the eastern half of Antarctica is a continent and the western half is an archipelago of islands bridged over by ice."

Traverse to Executive Committee Range

As part of the continuing US program in Antarctica, now under the direction of the National Science Foundation, an oversnow traverse to the Executive Committee Range, about 230 miles northwest of Byrd Station, was made by members of the station's scientific staff in February and early March of 1959. The traverse was led by John Pirrit, Station Scientific Leader at Byrd Station and Glaciological Project Leader for the 1959 Antarctic Program.

The party spent two days at the range

determining the positions of the peaks, making glaciological studies, and conducting a preliminary geological reconnaissance. Ten peaks were found in the range, the smallest reaching a height of 7144 feet above sea level and the largest reaching 13,856 feet. The range trends north-south for about 60 miles between about 76°20′S and 77°20′S and approximately along the 126°W meridian.

Preliminary geological investigations indicated that the mountains are volcanic in origin and are about 90% covered by snow and glaciers. Alpine-type valley glaciers flow from the peaks to join the vast ice sheet of Marie Byrd Land. Glacier action has eroded and modified the volcanic craters so that their original shapes are no longer recognizable. The high peaks are composed almost entirely of varieties of basalt overlaid by a thick series of volcanic breccias and tuffs. (Basalt is a fine-grained, dark, igneous rock commonly occurring as lava flows; breccias and tuffs are rocks formed of material ejected from volcanoes and subsequently compacted; the tuffs are fine-grained and the breccias are coarser and angular.)

An unusual and as yet unexplained finding was also made. Hundreds of black, partly rounded rocks of vesicular basalt (basalt containing cavities formed by gas bubbles when the rock was cooling) were discovered in one area. The rocks, generally 4–8 inches in diameter, were scattered over the surface of the ice sheet in the vicinity of several of the peaks. They were very numerous as far out as about two miles from the peaks, and isolated rocks were found as far away as approximately 17 miles.

The rocks were not distributed in the normal patterns characteristic of glacier deposits, or moraines; moreover, the glacier flow-rate was estimated to be not more than 50–100 feet per year, and many years would therefore have been required for the glaciers to move the rocks to their present positions. To further complicate the problem, the rocks do not show the alteration to be expected from differential rates of glacier flow, and appear to have been recently emplaced. Additional investigations will be required to determine how and when the rocks were deposited.

Position of IGY Amundsen-Scott South Pole Station

A more accurate determination of the geographic position of the IGY South Pole Station has recently been made. Computations based on 52 direct and inverted (to eliminate instrumental errors) theodolite observations of the star Canopus, from the station's astronomical loft, place the position of the loft at 89°59′43.6″ ± 0.7″ South Latitude, 24.8° ± 2.4° West Longitude. (Since the meridians of longitude converge at the poles, it is difficult to obtain the same apparent accuracy in longitude determinations at very high latitudes as in latitude determinations. However, only very small ground distances are involved so the actual accuracy is approximately the same.)

The Canopus observations were made between May 25 and July 6, 1958, by Palle Mogensen, then Station Scientific Leader at the IGY Amundsen-Scott Station, and the computations were performed by the Gravity and Astronomy Branch, Geodesy Division, of the US Coast and Geodetic Survey.

The astronomical loft is in the southernmost building of the station, which is laid out in a linear pattern roughly along the Greenwich Meridian and on the Greenwich side of the Pole. This latest determination places the position of the loft approximately 1650 feet from the geographic South Pole. It appears that the position is reliable to within 100–200 feet, exclusive of the "deflection of the vertical" (plumb-line deflection owing to gravity variations, as yet undetermined for the South Pole vicinity) at the observing site.

Firn Quakes

Two "firn quakes" were experienced by members of the oversnow traverse from IGY Byrd Station during the Antarctic summer of 1957–58. A firn quake is an icecap phenomenon somewhat resembling an earthquake but, by comparison, greatly limited in depth, areal extent, and severity.

These quakes are apparently confined to the firn—snow or granular ice that has lasted through at least one summer but has not yet become sufficiently compacted to be termed glacial ice. Firn reaches to depths of a few hundred feet in many places on the icecap. Firn quakes may be caused in several ways, but it is thought they frequently result from the collapse of widespread hoar-frost layers a few years old under the weight of overlying firn and snow.

Both quakes were felt during the third leg of the 1957–58 Byrd Station traverse. The first quake is believed to have occurred naturally, but the second was apparently triggered by an explosion set off in the course of seismic studies by members of the traverse party.

The first of the two firn quakes occurred about 90 miles southwest of the Sentinel Mountains, the turning point between the second and third legs of the traverse. The icecap in the region of the quake is about 5300 feet thick and the surface is about 6600 feet above sea level. The actual shock of the quake was preceded for about 10 seconds by a low, wind-like noise coming roughly from the direction of the Sentinel Mountains. The sound grew in intensity, as if approaching rapidly, until comparable to that of a jet aircraft passing overhead. The culmination of the phenomenon was a sharp, cracking sound accompanied by a sudden, distinct shock. No diminishing sound comparable to the pre-shock noise was noticed after the shock, and no indication of cracking could be found in the nearby ice surface. Moreover, examination of the walls of a three-meter snow pit excavated subsequently at the site of the quake disclosed no apparent collapse of any particular snow or firn horizon.

The second firn quake occurred about 170 miles farther along the traverse route two weeks later. At this point, an ice thickness of about 8600 feet and a surface elevation of 6700 feet were measured. The area was flat and featureless and about 65 miles west of the nearest mountains.

During seismic refraction studies, a member of the seismic team set off a 10-lb charge of explosives at a depth of about 13 feet in the snow cover and approximately 2.5 miles from camp. The shock that followed was greater than that ordinarily accompanying such an explosion. It was felt both by the scientist setting off the charge and by other members of the traverse party, 2.5 miles away. The noise preceding the quake, and the shock itself, were similar to those of the first quake, but this time the shock was followed by a receding noise in the direction opposite to that from which the pre-shock noise had come (the seismic shot point). Glaciologists working in a three-meter pit at the time of the quake observed no collapse of any of the snow or firn layers exposed in the pit walls.

Operation "Snuffles"

Work now is under way at Johns Hopkins University and the National Institutes of Health on hundreds of samples of blood sera, virus cultures, and bacterial cultures taken from US-IGY personnel in or enroute to and from the Antarctic.

The research is aimed at finding out more about the common-cold-like upper respiratory complaints. Answers are sought to questions such as these: Do the viruses associated with colds disappear from isolated groups? Do such groups lose their immunity to colds while sheltered from outside contacts? And the even more basic questions, exactly what causes the colds they catch, and how can these be counteracted?

Since isolated communities usually remain free from "colds" until visited by new people, the IGY Antarctic program provided an ideally controlled test situation.

The icebreaker *USS Staten Island* served as a floating laboratory for the project. All officers and men aboard gave samples of their blood at the beginning of the voyage and before their return to the US. In addition, 56 volunteers were studied closely throughout the entire voyage. Each gave a blood sample about once a month, and submitted to 15 throat swabs for virus cultures and 30 nose and throat swabs for bacteria. The specimens were collected mostly before and after visits to ports on the way south and in the Antarctic.

The information obtained aboard ship will indicate what infections were present in this semi-isolated community, and what infections could have been transmitted from it to the isolated and semi-isolated IGY Antarctic communities visited.

The *Staten Island* visited IGY Hallett Station (NZ-US), regarded as semi-isolated, and US-IGY Wilkes Station, which had been completely isolated for one year. Blood samples and swabs were taken from personnel of both stations.

Equipment was left at the Antarctic Research Laboratory, NAF McMurdo, for use in taking samples during the current Antarctic winter isolation. Samples also are being collected now at the South Pole, Hallett, and Wilkes Stations.

During the six-month voyage of the *Staten Island*, somewhat less than half the ship's company complained of "colds", many soon after leaving the various ports of call. From the swabs taken during these symptoms it is hoped to isolate some of the causal agents and match them with the antibodies later developing in the blood, or to differentiate them from true bacterial infections.

It remains to be seen if viruses found in the *Staten Island* volunteers can be picked up from personnel who joined the ship at Wilkes, or if the antibody experience of the Wilkes personnel parallelled that of ship personnel. Also significant will be the comparison of blood and swabs taken from Wilkes men before and after their isolation ended.

In its six months of operation, the *Staten Island* laboratory collected more than 900 samples of blood sera, more than 1300 virus cultures, and 2660 bacteria cultures.

To bring the sera and cultures back safely was a feat of logistics. It was necessary to maintain temperature for the virus cultures at a maximum of −60°C. The two freezers used for this purpose would not fit through the hatch, so a part of the metal bulkhead had to be removed and welded up again after the freezers were installed. When the ship returned to Seattle, the Air Force flew the freezers to Andrews Air Force Base, Maryland, in a C-97 cargo aircraft carrying two generators to provide the necessary emergency power.

William J. L. Sladen, the Project Director, assisted by Rainer Goldsmith of the Medical Research Council, London, was responsible for the field work. Sladen and others at Johns Hopkins University will work on the bacteriological material. Robert M. Chanock is doing the virus analysis at the Respiratory Virus Unit, National Institutes of Health.

J. W. Potter, Navy medical officer at NAF McMurdo, is continuing the investigation at the Antarctic Research Laboratory, and J. Boda, Australian medical officer, is doing likewise at Wilkes Station. "Operation Snuffies" also had the helpful cooperation of the Navy medical officers at Wilkes (R. Sparkes) and Hallett Stations (R. Bornmann and A. Bridgeman), and aboard the *USS Staten Island* (R. Duckworth) and *USS Glacier* (C. Stover). Australian, New Zealand, and British personnel also participated.

IGY Bibliographic Notes

This is the thirteenth of a series of bibliographic notes on IGY programs and findings. The references are selected largely from an IGY bibliography under preparation in the Science and Technology Division of the Library of Congress.

IA. L. Al'pert: Ionosphere Investigations by Artificial Earth Satellites. (In Russian). *Priroda.* No. 10, Oct. 1958. Pp. 71–77. Diagr.

R. V. Bhonsle and K. R. Ramanathan: Studies of Cosmic Radio Noises on 25 mc/s at Ahmedabad. *Journal of Scientific and Industrial Research.* Vol. 17a, no. 12. Dec. 1958. Pp. 40–45. Diagr., refs.

L. Biermann and R. Lüst: Radiation and Particle Precipitation upon the Earth from Solar Flares. *Proceedings of the IRE.* Vol. 47. Feb. 1959. Pp. 209–210.

Warren W. Berning: Earth Satellite Observations of the Ionosphere. *Proceedings of the IRE.* Vol. 47. Feb. 1959. Pp. 280–288. Illus., diagr.

R. L. Easton and M. J. Votaw: Vanguard I IGY Satellite (1958 Beta). *Review of Scientific Instruments.* Vol. 30. Feb. 1959. Pp. 70–75. Diagr.

John S. Farlow, III: *Project Ice Skate Oceanographic Data.* Woods Hole Oceanographic Institution. June 1958. 18 pp. Diagr. (Ref. No. 58–28).

Herbert Friedman: IGY Solar Flare Program and Ionizing Radiation in the Night Sky. *ARS Journal.* Vol. 29. Feb. 1959. Pp. 103–107. Diagr.

S. M. Greenfield and W. W. Kellogg: Weather Reconnaissance by Satellites. *Astronautics.* Vol. 4, No. 1. Jan. 1959. Pp. 32–33, 77–78. Illus., diagr.

Hugh Odishaw and Pembroke J. Hart: The International Geophysical Year World Data Center A. *News Report, National Academy of Sciences.* Vol. 8, No. 4. July-August 1958. Pp. 61–64.

B. Ramachandra Rao and E. Bhagiratha Rao: Effect of Enhanced Solar Activity on the F_2 Region Drifts at Waltair. *Journal of Scientific and Industrial Research.* Vol. 17A, No. 12. Dec. 1958. Pp. 59–62. Diagr., refs.

Report on the International Geophysical Year. (Hearings Before the House of Representatives Committee on Appropriations, Subcommittee on Independent Offices.) Washington, Government Printing Office. 1959. 110 pp.

Henry L. Richter, Jr., William Pilington, John P. Eyraud, William S. Shipley, and Lee W. Randolph: Instrumenting the Explorer I Satellite. *Electronics.* Vol. 32, no. 6. Feb. 6, 1959. Pp. 39–43. Illus., diagr.

Milton Rosen: What We Have Learned from Vanguard. *Astronautics.* Vol. 4, No. 4, Pt. 1. April 1959. Pp. 28–29, 110–111. Illus., diagr.

Alan H. Shapley: The Day-to-Day Coordination of IGY Observations. *Proceedings of the IRE.* Vol. 47. Feb. 1959. Pp. 323–327.

W. G. Stroud: Meteorological Rocket Soundings in the Arctic. *Jet Propulsion.* Vol. 28. Dec. 1958. Pp. 817–822. Diagr.

Submerged "River" Found in Pacific. *Journal of Geophysical Research.* Vol. 63. Sept. 1958. Pp. 558–559.

J. O. Thomas: The Distribution of Electrons in the Ionosphere. *Proceedings of the IRE.* Vol. 47. Feb. 1959. Pp. 162–175. Diagr.

Vol. 40, No. 3 TRANSACTIONS, AMERICAN GEOPHYSICAL UNION September 1959

NATIONAL ACADEMY OF SCIENCES

Number 27 • September 1959

IGY BULLETIN

A monthly survey of programs and findings of the International Geophysical Year and the International Geophysical Cooperation–1959 as related primarily to United States programs

The Argus Experiment

The following report is based primarily on papers presented at the Symposium on Scientific Effects of Artificially Introduced Radiations at High Altitudes, held at the National Academy of Sciences, Washington, D. C., on April 29, 1959. The papers, which appeared in complete form in the August 1959 issues of both the Proceedings of the National Academy of Sciences *(reprinted also as* IGY Satellite Report Series No. 9, *September 1959) and the* Journal of Geophysical Research, *were, in the order of their presentation, read by Richard W. Porter of the General Electric Company, Nicholas Christofilos of the University of California, James A. Van Allen of the State University of Iowa, Major Lew Allen, Jr., and Captain Joseph A. Welch, Jr., of Kirtland Air Force Base, New Mexico, Philip Newman of the Air Force Cambridge Research Center, and Allen M. Peterson of Stanford University.*

Although the Argus Experiment was not part of the IGY Program, and neither the USNC-IGY nor the National Academy of Sciences was instrumental in its planning and conduct, an IGY satellite made many observations of Argus phenomena. Moreover, Argus data relate to upper-atmosphere work investigated in IGY programs. Hence, the experiment appeared to be of sufficient interest to IGY scientists to warrant this summary report in the Bulletin.

Equipment for measuring cosmic-ray intensity at high altitudes, carried in US-IGY satellite 1958 Alpha (Explorer I), first discovered the existence of high-intensity radiation—the Van Allen radiation regions—trapped in the earth's magnetic field. (In this report, the term "radiation" in general refers to charged particles.) Further investigations with 1958 Gamma and 1958 Epsilon (Explorers III and IV, respectively) and with the US-IGY deep-space probes, Pioneers I, III, and IV, increased knowledge of the nature of the radiation and its extent in space. (*See Bulletin No. 21.*)

The manner in which charged particles are trapped in the earth's magnetic field has been long understood through the work of C. Stoermer, H. Alfven, and others. This theory was confirmed by the satellite and space-probe observations mentioned above.

In October 1957, a few months before the launching of 1958 Alpha, N. C. Christofilos, of the University of California's Lawrence Radiation Laboratory, noted that many observable geophysical effects could be produced by small-yield atomic detonations in the earth's tenuous upper atmosphere.

It was believed by Christofilos and upper-atmosphere physicists to whom the idea was communicated, that artificial, impulsive injection of known particles along known magnetic lines of force, at a known time would constitute a powerful technique for clarifying uncertainties of the dynamics of geomagnetic trapping as well as for studying related geophysical effects. The

natural radiation trapped in the Van Allen regions could not, of course, be subjected to such experimental control.

Theory: According to the trapping theory, an electron injected at high altitude into the earth's magnetic field, which closely resembles that of a bar magnet, would spiral in a helical pattern about a magnetic line of force (see Fig. 1). Since the field

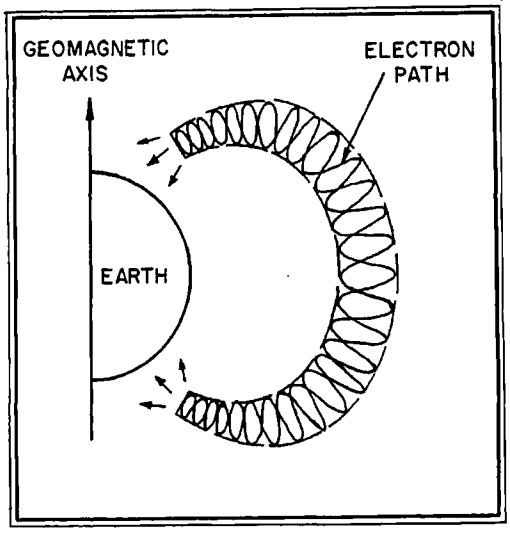

FIG. 1. *Schematic Diagram of Path of Electron in the Earth's Magnetic Field. (Actual path is very much narrower and describes innumerable tight spirals.) Angular distributions at the mirror points form disc-like patterns. Most electron losses occur by scattering in the denser atmosphere near the mirror points.*

strength increases toward the earth, the particle would finally reach a point near the end of the line of force, but still at considerable height, beyond which it could not penetrate. These points, one of which exists for each particle at each end of the line of force about which it spirals, have been termed "mirror points" since they cause the particle to be reflected back along its course. This process continues at great speed until the particle is finally "lost," usually in the vicinity of the mirror points, through repeated collisions with molecules of the earth's atmosphere.

In addition to the motions described above, trapped electrons would drift eastward around the earth owing to the decrease in strength of the magnetic field with altitude, the centrifugal force of the spiraling particles, and certain other factors. Hence, if a sufficiently large volume of electrons were injected into the magnetic field at a single point, the combined motions would result in the formation of a thin shell of electrons completely encircling the earth and bounded approximately by the magnetic lines of force between which the particles were injected.

The lifetime of an electron trapped in the magnetic field is directly proportional to the length of the line of force about which it spirals and approximately to the square of the electron's energy, and inversely proportional to the air density at the mirror points. Injected electrons would be scattered out of their initial spiral trajectories by collisions with air particles, and, since the density of the atmosphere decreases exponentially with increase of altitude, such collisions would occur with greatest frequency near the mirror points, in the lower portions of the electron paths. Hence, most electron losses would occur near the mirror points. The scattering results in further lowering of the mirror points into regions of still greater density. It was expected that most electrons with energies of 1-2 million electron volts (mev) injected at an altitude of a few hundred kilometers would survive for several hours or more.

In addition to the trapping effect, the creation of an artificial aurora at each end of the lines of force passing through the detonation region was predicted. Electrons from the detonation would be guided along these lines of force in both directions, ionizing the air through which they passed and also causing auroral luminescence at both points where the lines of force re-enter the denser atmosphere. It was also expected that certain magnetic, electromagnetic, and ionospheric effects would be observable.

Organization of Experiment: After preliminary calculations had been made by

Christofilos, a proposal for a series of studies based on the artificial injection of electrons into the magnetic field at high altitudes by small-yield nuclear detonations was presented to the President's Science Advisory Committee. At the suggestion of this committee, a group of representatives of both the scientific and military communities (since the experiments involved the interests of both) was formed to appraise all aspects of the undertaking. By this time, the IGY satellite experiments designed by James A. Van Allen of the State University of Iowa had partially confirmed the trapping theory. Therefore, it was decided late in April 1958 to proceed with the artificial-injection experiment, which was given the code name of "Argus." Overall responsibility for the preparation and conduct of the Argus Experiment was given to the Advanced Research Projects Agency (ARPA) of the Department of Defense. Herbert York, then Chief Scientist for ARPA, directed the program.

Since the magnetic axis of the earth is tilted with respect to the axis of rotation and the center of the magnetic dipole is displaced toward the Pacific Ocean, it was apparent that the mirror points would be closest to the earth's surface over the South Atlantic. Hence, this region was selected for the high-altitude detonations. This location also afforded conjugate, or mirror, points near the Azores Islands in the North Atlantic, making it easier to conduct observations of the aurora expected to occur at that end of the line of force.

The mission of delivering three small-yield nuclear devices to high altitude over the South Atlantic and detonating them was undertaken by a US Navy task force specially organized for this purpose. The three nuclear devices were detonated in late August and early September 1958, all at a nominal altitude of 480 kilometers (about 300 miles). They were delivered to their detonation points in the upper atmosphere by multi-stage rockets launched from the *USS Norton Sound*. The first burst occurred at approximately 0230 UT, August 27, at a geographic location of approximately 38°S, 12°W; the second was at about 0320 UT, August 30, near 50°S, 8°W; and the third was on September 6, at about 2210 UT, and in the vicinity of 50° S, 10°W. The position of the shells of trapped Argus electrons relative to the Van Allen regions of trapped natural radiation is shown in Figure 2.

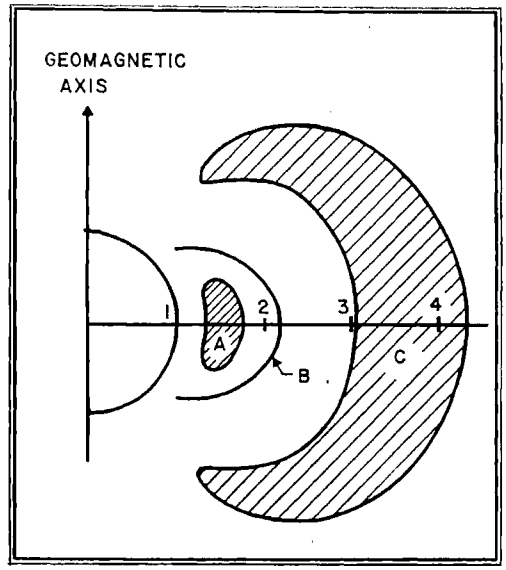

Fig. 2. *Approximate Position of Argus Shells with Respect to the Van Allen Regions of Trapped Natural Radiation. A is the inner Van Allen belt; B is the position of the Argus shells; and C is the outer Van Allen belt. Scale in earth radii.*

Two IGY satellites, Explorer IV (1958 Epsilon) and Explorer V, contained instrumentation designed at the State University of Iowa to measure the natural radiation in the Van Allen belts. This instrumentation was also capable of measuring the artificial radiation in the Argus shells. (Explorer V did not go into orbit.) The Air Force Special Weapons Center prepared a series of high-altitude sounding rockets to study the lower fringes of the radiation shells (Project Jason). Stanford Research Institute and the Air Force Cambridge Research Center developed and installed at various ground locations and aboard aircraft and ships a

variety of equipment to measure the expected auroral, radio, magnetic, and electromagnetic effects. The following material reviews the aims, techniques, and preliminary results of the various investigations related to the Argus Experiment.

Satellite Observations

1958 Epsilon entered an orbit inclined at 51° to the equator at 1506 UT, July 26, 1958 (see *Bulletin No. 15*). The instrumentation it carried (Table 1) was designed under the direction of James A. Van Allen, Carl E. McIlwain, and George H. Ludwig, all of SUI.

Table 1. Summary of Detector Characteristics (Explorer IV)

Channel	Detector	Shielding	Sensitive to:	Geometric Factor
1	Geiger-Mueller Counter (Anton 302); cylinder approximately 7 mm × 9 mm; scaler: 64	1.2 g/cm² Fe + 1.6 g/cm² Pb (minimum)	Electrons of $E >$ 5 mev; protons of $E >$ 40 mev; X-rays of $E >$ 80 kev, with low efficiency	Omnidirectional geometric factor 0.14 cm² for minimum stopping power; 0.82 cm² for penetrability greater than 7 g/cm²
2	Plastic scintillator—0.76 cm. diameter, 0.18 cm thick; pulse detector; scaler: 16	0.14 g/cm² of aluminum over window	Electrons of $E >$ 580 kev; protons of $E >$ 10 mev; axis of detector ⊥ to payload axis; X-rays of $E >$ 300 kev, with low efficiency	0.040 cm² steradian for minimum stopping power; 4.2 cm² steradian for penetrability greater than 5 g/cm²
3	Same as Channel 1 except less shielding; scaler: 2048	1.2 g/cm² Fe (minimum)	Electrons of $E >$ 3 mev; protons of $E >$ 30 mev; X-rays of $E >$ 20 kev, with low efficiency	Omnidirectional geometric factor 0.14 cm² for min. stopping power; 0.70 cm² for greater than 5 g/cm² stopping power
4	Cesium Iodide crystal — 0.76 cm diameter, 0.20 cm thick; total energy-d.c. electrometer	1.0 mg/cm² of nickel and aluminum over window	Electrons of $E >$ 20 kev; protons of $E >$ 400 kev; X-rays; axis of detector ⊥ to payload axis	0.0235 cm² steradian for minimum stopping power; 4.4 cm² steradian for penetrability greater than 5 g/cm²
5	Same as 2 except scaler: 2048			

The location in space of the magnetic shells created by the experiment was chosen so that the shells could be intercepted by a relatively low-altitude satellite with an orbital inclination not greater than 51°, the highest inclination practical with the available facilities. The intermediate latitude chosen for the detonations also permitted the satellite orbit to intercept the shells of trapped particles at a less oblique angle. Moreover, since the measurements of Explorers I and III had shown a rapid decrease with distance from the magnetic equator in the intensity of the natural radiation at a given altitude, the "background" radiation was expected to be less at intermediate latitudes than at lower latitudes.

Nature and Scope: In the month before Argus I, 1958 Epsilon collected much data serving to establish the detailed spa-

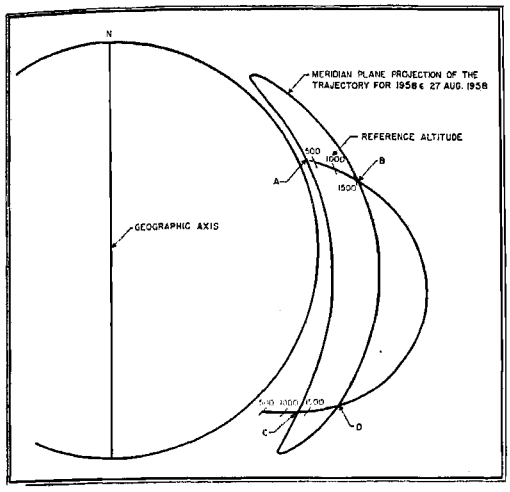

Fig. 3. *Typical Geometric Relationships Between 1958 Epsilon Orbit and Argus Shells. A, B, C, and D represent points of intersection; reference altitudes are in kilometers.*

tial relationships and many of the properties of the natural trapped radiation. Between August 27 and September 19, significant data were obtained on 164 intersections of the Argus shells by 1958 Epsilon. Most of the observed intersections occurred in the northern hemisphere, where tracking facilities are more complete.

Typical geometric relationships between the satellite orbit and the shell of magnetically trapped radiation are shown schematically in Figure 3. It can be seen that ideally the shell is intersected four times, at various altitudes, latitudes, and longitudes, during a satellite revolution. Actually, however, significant data were obtained on an average of much less than four intersections per orbit owing to the low altitude, and hence the low electron intensity, of many intersections; distortion and tilt of the magnetic shell, so that fewer than four intersections occurred on some orbits; occurrence of some intersections beyond radiotelemetry range of the receiving stations; and occurrence of some intersections at points where the intensity of artificial radiation was smaller than that of the natural radiation (this condition prevailed everywhere along the satellite orbit after each artificial-radiation shell had decayed with time to a certain degree).

The lower-powered of the two transmitters and telemetry channels 2 and 5 were exhausted on about September 3. The higher-powered transmitter and channels 1, 3, and 4 operated properly until about September 21. By this time the Argus III particles were still being detected above the background radiation, but only on occasional favorable intersections. It appears, however, that space-probe Pioneer III (see *Bulletins 20 and 21*) detected a residuum of Argus electrons near the geomagnetic equator on December 6, 1958, but none were detected in this region by space-probe Pioneer IV on March 3, 1959.

The "Argus effect" was easily and promptly observed by 1958 Epsilon after each of the three detonations. Figure 4

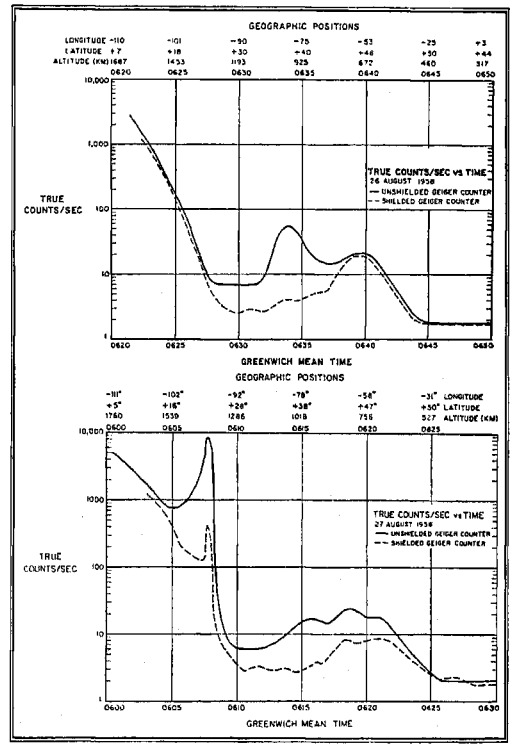

Fig. 4. *Comparison of Counting Rates the Day Before Argus I (upper graph) and a Few Hours After Argus I. The peak at 0608 UT on the lower graph represents intersection of the electron shell by 1958 Epsilon.*

shows a record of measurements of the natural radiation taken the day before Argus I (upper graph), and a record taken through a similar geographic region about 3½ hours after the Argus I detonation (lower graph). Nothing equivalent to the great peak intersected at 0608 UT, August 27, had been observed by 1958 Epsilon during the preceding four weeks. Moreover, the peak was encountered on the first observed intersection with the planned magnetic shell following the Argus I burst. During the entire active period of 1958 Epsilon (July 26-September 21, 1958) no such peaks were observed except those corresponding in time and place to the expected artificial radiation.

Further reasons for identifying these peaks with the Argus effect are: the observed energy spectrum and the nature of the radiation agreed essentially with those expected for decay electrons from fission fragments; a similar peak was found at every observed intersection throughout the experiment, regardless of geographic location; geometric thickness of the shell, measured electron intensity, and decay time of the intensity of the artificial radiation resembled pre-test estimates.

Figure 5 is a record made on August 31

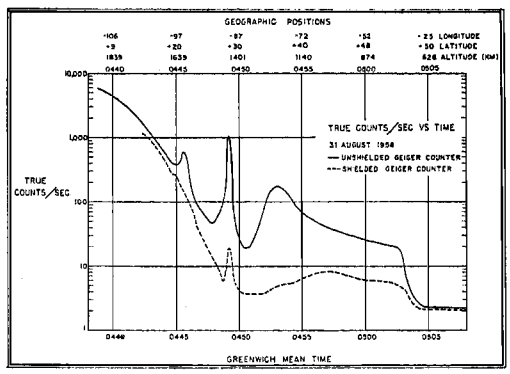

Fig. 5. *Counting Rate Record Showing Fresh Argus II Peak and Decaying Argus I Peak. Large peak at 0449 UT represents satellite intersection of Argus II shell; small peak three minutes earlier is intersection of remnant of Argus I shell.*

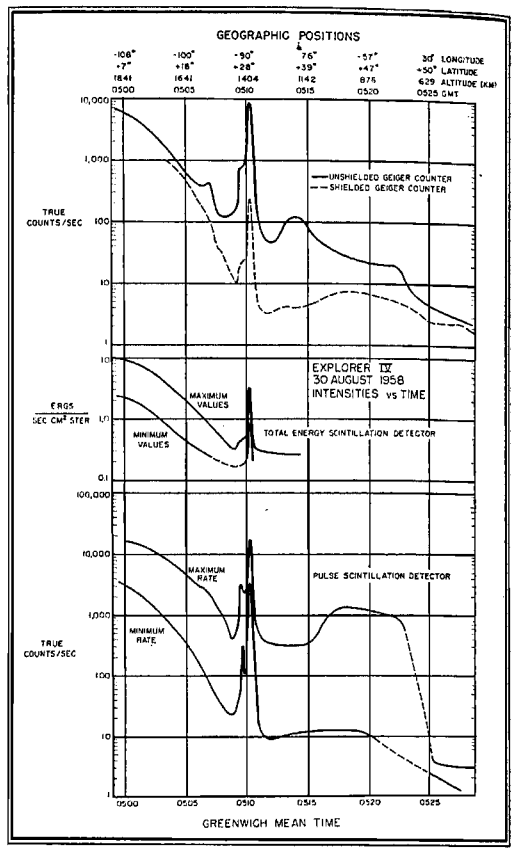

Fig. 6. *Comparison of Geiger Counter and Scintillator Records Showing Intersection of Argus Shells by 1958 Epsilon on August 30, 1958.*

showing the decaying peak (0446 UT) of the Argus I radiation and the fresh peak (0449 UT) resulting from the Argus II detonation. Plots of the reduced and corrected data from all four detectors for an intersection on August 30 are shown in Figure 6.

The angular motion of the satellite as it rolled and tumbled through the electron shell, apparent in the instrumental records, was advantageous for the measurement of angular distributions of the Argus electrons. These distributions, as observed near the mirror points, were found to form disc-like patterns (Fig. 1), as previously suggested by the magnetic-trapping theory and as observed extensively in studies of the natural radiation.

In each set of observations, the output of each detector was converted either to true counting rate (channels 1, 2, 3, and 5) or to absolute directional energy flux (channel 4), using pre-flight calibration data. From the corrected plots, estimates were made of net intensity of Argus electrons above background; "time width" of the Argus peak between points of half-maximum intensity and between points of 1/10 maximum intensity; local maximum and minimum intensities near the center of the peak; and time of occurrence of the center of the peak. Then, using the ephemeris of 1958 Epsilon, tabulations were made of the latitude, longitude, and altitude of the center of the peak, and of the geometric thickness of the shell at half-maximum intensity, measured perpendicular to the shell.

Preliminary Summary of Results: Based on the data collected by 1958 Epsilon during its intersections of the Argus shells, certain preliminary results have been obtained regarding the shells, the nature of the electrons, and the geomagnetic field.

The mean thickness, at half-maximum intensity and measured perpendicular to the shell boundaries, of the Argus I and II shells was about 90 kilometers, and the mean thickness of the Argus III shell was about 150 kilometers. The thickness did *not* depend systematically on elapsed time, (except possibly during the magnetic storm on about September 4; see below), but the measured values show a scattering of about 30%. The investigators assume that the basic shell thickness was determined by the very complex injection situation at and immediately following each detonation. This surmise is supported by rough calculations of the dynamics of the detonations in the earth's magnetic field.

The magnetic shells reached outward about two earth radii from the center of the earth. The leakage of particles from the ends of the shells and by energy loss proceeded at a sufficiently rapid rate so that, in general, diffusion across the boundaries of the shells was too slow by comparison to be observed.

Plots were made in which each observation of the center of each Argus shell (I, II, and III) was projected downward to the surface of the solid earth by use of a simplified model of the geomagnetic field (the eccentric dipole model, in which the magnetic axis does not correspond to the geographic axis). The three resulting loci of points, interlaced in time, are notably smooth and regular, suggesting positional stability of the shells during the observing period. It was concluded that the shells could not have drifted in latitude by more than about 0.03° per day (about 2 kilometers per day at a height of 1500 kilometers) without having resulted in a "ripple" in the implied geomagnetic field contour not supported by other data.

The disc-like character of the angular distribution of the trapped electrons, and the angular thickness of $\pm$ 20° or less, show that at the relatively low observational altitudes most particles measured had turning points (or mirror points) not more than a few hundred kilometers below the locations of the observations. This is quite reasonable in terms of the basic dynamics of magnetic trapping.

The maximum observed intensity at the center of the shell multiplied by the thickness of the shell at half-maximum intensity has been taken as a measure of the total intensity of trapped particles (within the range of the detector used). Several preliminary plots of this quantity against elapsed time were made for two different possible positions in the geomagnetic field. Examination of these plots, and application of a theory by Ernest C. Ray of SUI on the loss mechanism for particles trapped in the magnetic field, permits estimates of the time-decay of the intensity of the trapped radiation. These estimates pertain to an effective electron energy of 3.5 mev. Ray computed the effective atmospheric density, for an altitude of 1000 kilometers, that

would be required to reduce the radiation intensity as rapidly as observed. He found this density to be least 10 times as great as that reached by extrapolation from an atmospheric model derived by Robert Jastrow from studies of atmospheric drag on satellites. The SUI workers believe it is possible that atmospheric density is anomalously high in the region of the Argus shells, which occurred in the "slot" between the two zones of trapped natural radiation (Fig. 2).

An alternative speculation is that the rapid decay was caused, in part at least, by "magnetic diffusion" owing to small-scale and perhaps time-dependent irregularities of the geomagnetic field. Investigation of this possibility is in process, using the results obtained from all four detectors, which were designed for different effective particle energies.

. The gross decay rate is presumably a composite of atmospheric and magnetic effects.

A discontinuously rapid drop in intensity of the Argus I and Argus II radiation on about September 4 suggests that a very large magnetic storm on that date may have caused great enhancement of the rate of loss of stored particles. Also, the Argus II shell appears to have thickened significantly during this period.

The 1958 Epsilon observations permit estimation of the total number of trapped Argus electrons having turning points below the highest altitude of observation. This estimate, made as of zero elapsed time, serves to supply a lower limit to the fraction of electrons effectively injected into the geomagnetic field, since the nominal yield of the injection and the nominal energy spectrum of the electrons are known.

When the product CWt (maximum intensity at the center of the shell × thickness × time) is plotted against the strength of the magnetic field in the region occupied by the shell, it can be seen that there is an increase in the density of turning points with increasing altitude (i.e., with decreasing field strength). It is therefore evident that injection of the longer-lived electrons occurred largely at altitudes much greater than that of the detonations.

As a result of observations of satellite 1958 Epsilon, the geometric form of the Argus shells is known to a precision of about ± 10 kilometers with respect to the earth. Hence, these experiments provide a significant new method for the harmonic analysis of the general geomagnetic field. Although this analysis is not yet complete, it is already clear that at least the dipole and quadrupole terms of the magnetic field can now be determined with useful accuracy.

Optical, Radio, and Magnetic Observations

Because it was expected that the Argus detonations might result in optical, radio, and magnetic effects that could be observed from ground level, the Stanford Research Institute and the Air Force Cambridge Research Center cooperated in a program to measure these effects. The techniques used and some of the results of these experiments are described below.

Aurora: The auroral luminescence resulting from the Argus detonations was observed at both the detonation site and the conjugate point in the northern hemisphere by visual observers, all-sky cameras and other photographic methods, and by radar. In addition, photometers and interference filters were used to study the spectrum of the artificial auroras.

In the detonation area, all three events were accompanied by colorful auroras elongated along a line intersecting the magnetic meridian at an angle of 10°. Photometric records were obtained for each event at the 5577 A and 3914 A wavelengths of the auroral spectrum. (The former is the green line of atomic oxygen and the latter is one of the violet lines of nitrogen.) The ratio of atomic oxygen to nitrogen, about 10:1 for

the third Argus event, was much higher than that usually observed in natural auroras.

The investigators assume that the auroral effect was caused mainly by the strong excitation by fission products of oxygen and nitrogen at the 100-kilometer level in the earth's atmosphere. The photometric records also serve as a check on the detonation time.

In the conjugate area, near the Azores Islands, only one doubtful sighting was made after Argus I and none was made after Argus II. After the third detonation, however, a brilliant auroral display was observed by many members of the crew of the *USS Albemarle* and by civilian scientists aboard. Distances to the conjugate aurora resulting from Argus III, estimated by observers aboard the *Albemarle,* correspond to auroral heights of about 240–565 kilometers. Visual estimates of its duration ranged from about 5 to about 30 minutes.

Radar echoes were returned from all three of the auroras in the detonation area and from auroras accompanying Argus I and III at the conjugate point. In the detonation area the echoes appeared within seconds after the burst. In one case, these echoes were observed for five hours. In the conjugate area, echoes appeared somewhat later, but still within a minute of the burst, and lasted in one case for an hour and 15 minutes. The radar observations in the conjugate region agree approximately with the auroral height estimates based on the visual observations, and, in combination with the visual observations, located the conjugate point within about 100 kilometers of the theoretically expected location.

Magnetic and Electromagnetic Studies: It was expected that a detonation of the Argus type would cause a shock wave in the atmosphere which would be propagated as a hydromagnetic wave, or Alfven wave, along the magnetic line of force. This effect would be detectable on the ground by very-low-frequency (VLF) equipment or by magnetometers. A change in the magnetic field might result from the hydromagnetic wave or from an electric current in the atmosphere.

Several types of equipment were available in the Azores to monitor these effects. Extremely-low-frequency (ELF) instrumentation (0.3 to 30 cycles/sec) was set up to measure changes in the magnetic field. Also used were a heliflux magnetometer and a variable-mu magnetometer to measure the static field. Regular magnetic stations, as well as IGY aurora and air glow stations, were also available to observe detonation effects. Similar equipment, with the exception of the ELF apparatus, was installed on ships in the detonation area.

The ELF receiver in the conjugate area obtained results for the second and third detonations, but not for the first. (Argus I took place during a geomagnetic disturbance accompanied by unusually severe radio blackout. Moreover, the magnetic lines of force within which Argus I took place, and along which these effects presumably would be propagated, may have passed through or near the lower of the Van Allen radiation regions.)

ELF signals received after the Argus II and III detonations were unmistakably distinguishable from background electromagnetic effects. Harmonic analyses indicated signal components between about ½ and 2 cycles/second. Estimates of changes in amplitude of the various magnetic-field components ranged from about 1/25 to 3/2 gamma, with the largest changes generally occurring in the east-west component of the field and the smallest in the vertical component.

The ground speed of propagation of a strong disturbance (at plus 42 seconds) from the detonation point was about 700 km/sec. If it is assumed that the disturbance followed the magnetic line through the detonation point, its average speed along the line of force would be about 2000 km/sec.

A magnetic detector in the launch area recorded an initial one-second-pulse signal of about one cycle/sec for Argus III with a strength of more than 10 gammas, followed by longer-period pulses. The total duration, with irregular fluctuation, was about 1½ minutes.

Radio Propagation: Variations in propagation characteristics of radio waves in the very low frequency (VLF) range—300 cycles/sec to 30 kilocycles/sec—have for many years been recognized as sensitive indicators of lower-ionosphere conditions (below about 100 kilometers). The VLF signals can be enhanced by increased ionization at the normal heights of reflection of the radio waves; on the other hand, if ionization is increased at lower levels, where atmospheric density is greater, absorption results and signal strength is reduced.

For the Argus experiments, VLF equipment similar to that used during the IGY for whistler studies (see *Bulletin No. 6*) was designed, constructed, and installed by the Stanford University Radio Propagation Laboratory. Recordings were made with this equipment in the launch area, at several locations in the conjugate area, and at Stanford University, California.

Of particular interest were recordings made in the Azores and in Spain of signals at a frequency of 19.6 kilocycles/sec from station GBZ in England. These recordings showed abrupt decreases in signal strength of 6-12 decibels following Argus II and III. Recordings made at Stanford University of signals from stations NPG in Seattle (18.6 kilocycles/sec) and NDT in Japan (17.1 kilocycles/sec), on the other hand, showed slight increases in signal strength for some minutes following Argus II and III.

A possible explanation for the observations in the conjugate area is that electrons scattered from the magnetic shells, as well as the ionized debris itself, may have penetrated to low altitudes, increasing the ionization in the lower ionosphere and producing absorption. In the Pacific, far removed from the original injection region, the enhancement of signal strength may indicate increased ionization at higher levels above the earth.

Radio Noise: As part of the Argus measurements, three riometer stations were operated near the conjugate region at frequencies of 30, 60, and 120 megacycles/sec, and one was operated near the launch area at 30 megacycles/sec. (The riometer is designed for sensitive routine measurement of ionospheric absorption by monitoring the power level of cosmic noise propagated through the ionosphere.)

Although the perturbation of the ionosphere by the Argus detonations was sufficient to reduce, by absorption, the strength of VLF signals (see above), it was not large enough or widespread enough after any of the three Argus detonations to be detected by the riometers.

Another purpose of the riometer network was to provide a sensitive measure of radio noise that might be generated by electrons trapped in the Argus shells. Noise from this source was not detected, and, on the basis of particle-counting data from 1958 Epsilon during the Argus Experiment and of comparison of electron density in the Argus shells with counting rates in the Van Allen regions, it is now believed that this radio noise should, in fact, have been below the detectable level. However, the experiment showed that such radio noise information might reasonably be extracted, in the future, by careful radio astronomy methods.

Jason Rocket Observations

The "Jason" project, conducted by the Air Force Special Weapons Center, consisted of the launching of 19 high-altitude rockets carrying instrumentation to measure the electron flux of the Argus shells. The rockets were sent to altitudes of about 800 kilometers from Cape Canaveral, Florida, Wallops Island, Virginia, and Ramey Air Force Base, Puerto Rico. The

sites were chosen to provide sufficient latitudinal coverage to assure interception of the shells. The instrumentation in each rocket consisted of eight Geiger-Mueller counters with various amounts of shielding to provide an energy scale and various orientations to provide directional information. Data were telemetered to ground stations. Thirteen successful flights were made, one for pre-Argus background data, two following Argus I, and 10 following Argus II.

Only limited data were obtained from the Argus I flights, but much information resulted from the flights following Argus II. Rockets launched southward from Wallops Island observed a narrow region in which counting rates were very high—initially, 100,000 times normal. The rockets penetrated the Argus II shell at altitudes of about 320 to 485 kilometers, and the shell was observed to be about 20 kilometers thick in this region. Increases in radiation level were observed about 700 kilometers to the north and to the south. Both the width and the position of the shell remained constant (± 8 kilometers) throughout the 100-hour observation period. This extreme constancy, while the electrons traveled from north to south more than 1,000,000 times and drifted around the world more than 100 times, verifies many important hypotheses about the earth's magnetic field and the character of space as far out as one earth radius from the surface.

The intensity of trapped electrons in the shell was observed to be approximately inversely proportional to the time from the burst. This is consistent with the theory that the trapped electrons are lost predominantly through scattering in the atmosphere near the mirror points.

Measurements of angular distribution of the electron flux, based on determination of the orientations of the rocket instrumentation by analyzing telemetry signal-strength records, show that the flux was confined to a plane very nearly perpendicular to the lines of force of the magnetic field.

Conclusions

A great variety of measurements of the magnetically trapped radiation from the Argus detonations were made by special instrumentation included in the payload of IGY satellite 1958 Epsilon and by rockets and ground-based equipment employed by various agencies. Preliminary analyses have confirmed the theory of trapping of radiation by the magnetic field of the earth and have supplied new information about the configuration and some of the characteristics of the magnetic field. Data gained by this controlled experiment, in which many of the factors were known, may also provide an improved basis for understanding the mechanics of the natural trapping of charged particles in the Van Allen radiation regions, and of related phenomena such as the aurora.

Oversnow Traverses from IGY Little America Station

The following material was prepared by Albert P. Crary, leader of the traverses described and Station Scientific Leader at Little America Station during 1956–57 and 1957–58.

Three oversnow traverses were made inland from Little America Station during the International Geophysical Year. (Figure 7 shows the routes of these three traverses and of others made during the IGY.)

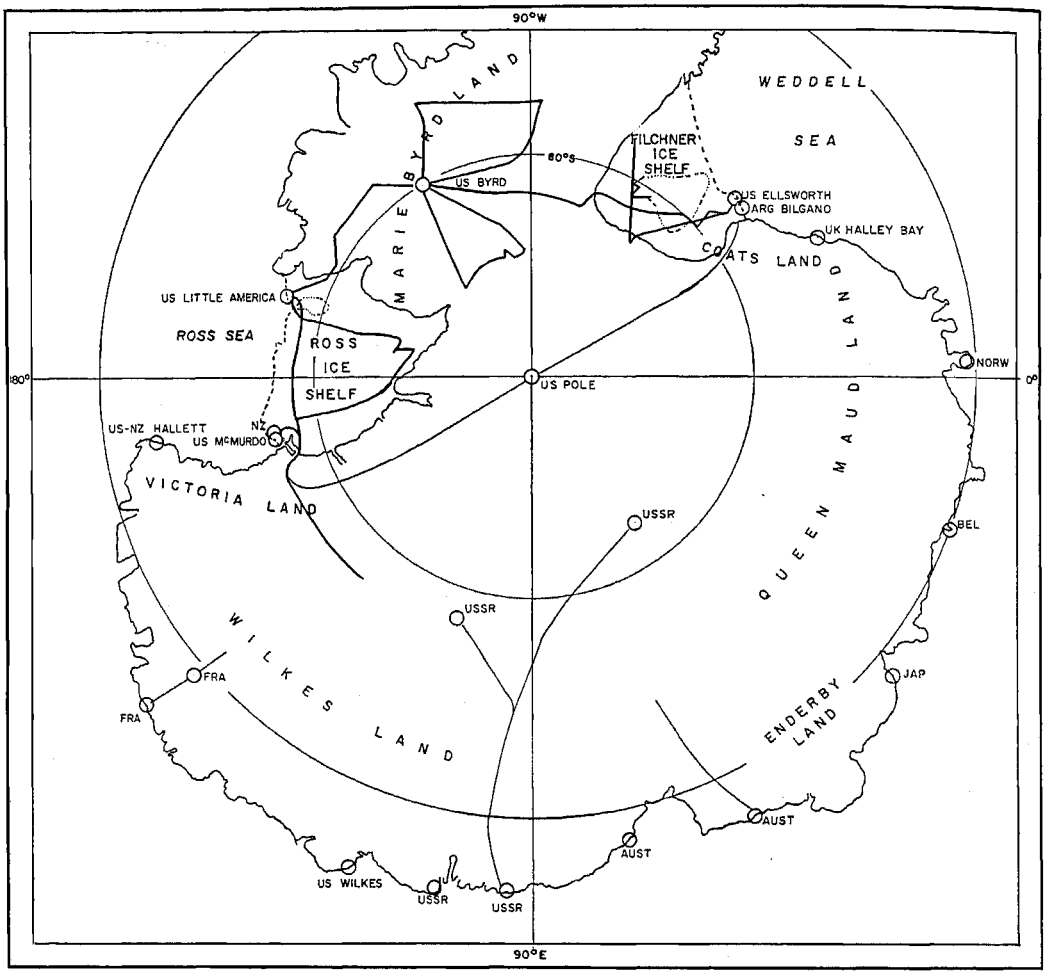

FIG. 7. *Antarctic Traverses During IGY. Treated in this report are those made from US-IGY Little America Station on the Ross Ice Shelf during 1957–58, and in the following year from Little America across the Ross Ice Shelf up the Skelton Glacier and along the Victoria Land Plateau.*

The Ross Ice Shelf Traverse, from October 24, 1957, to February 13, 1958, covered a total of about 1225 nautical miles. (A preliminary description of this traverse is given in *Bulletin No. 10.*)

The Byrd Tractor Trail Traverse was made from March 25 to April 10, 1958. The party traveled along the Little America-Byrd Station tractor trail for 140 nautical miles, to a point close to the junction between the floating and grounded ice.

The Victoria Land Traverse started on October 15, 1958, at Little America Station and ended January 31, 1959, at Scott Base (NZ) on Ross Island in McMurdo Sound. The first part of this journey duplicated the first leg of the Ross Ice Shelf Traverse of the previous year. On this stage, a few additional observations were made in some areas where the 1957–58 water depth and gravity readings departed from computed norms. The standard program of closely spaced observations, including data needed for glacial regime studies, started as the party left the earlier route and headed west to the Skelton Inlet, a few miles south of the Minna Bluff-Mount Discovery peninsula.

A month was spent moving from the shelf ice up the Skelton Inlet and the Skelton Glacier to the Victoria Land plateau. From the top of the plateau at the head of the Skelton Glacier, the traverse party traveled due west. It followed a line a few miles south of 78°S for about 350 nautical miles to 131.5°E. The party then returned along the same route, making stops on the Skelton Glacier and on the western Ross Ice Shelf to remeasure snow accumulation and ice movement at stakes installed on the outward journey. From Minna Bluff to Scott Base a detailed seismic-sounding and ice-movement program was undertaken.

A large portion of the data taken on these traverses is still in the process of reduction and analysis. This report describes some preliminary results of the studies on the Ross Ice Shelf and in Victoria Land.

Ross Ice Shelf

Study of the Ross Ice Shelf was included on all three of the traverses. Figure 8 shows tentative ice thicknesses; the elevation of the surface above sea level was generally 1/7 to 1/8 of the ice thickness. The general thickening of the shelf along the southeastern part (upper left in Fig. 8) is indicative of the large contribution to the nourishment of the shelf made by the southwestern part of Marie Byrd Land and the polar plateau, as compared with that of the glaciers along the western part of the shelf. Near the junction of the floating and grounded ice in the Skelton Inlet (lower right in Fig. 8), floating ice is nearly 1000 meters (approximately 3280 feet) thick.

Figure 9 gives preliminary findings on water depths, with some data from US Navy Hydrographic Office charts added for the waters off the barrier edge. The deep waters around the periphery of the shelf, and the particularly deep sounding due south of Mount Discovery, are noteworthy. A few soundings even deeper were made in the Skelton Inlet, a distinct fiord with deep

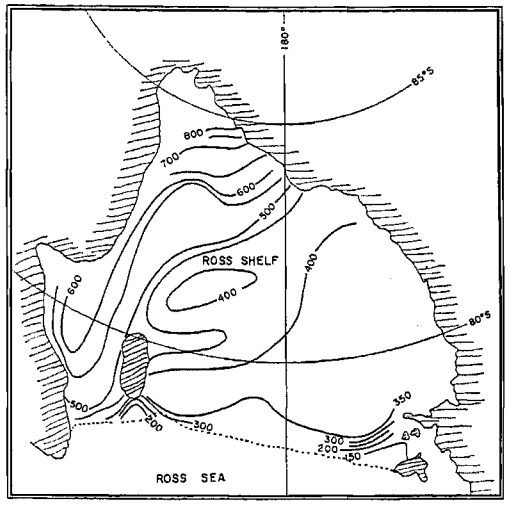

FIG. 8. *Thickness of Ice Shelf in Meters.*

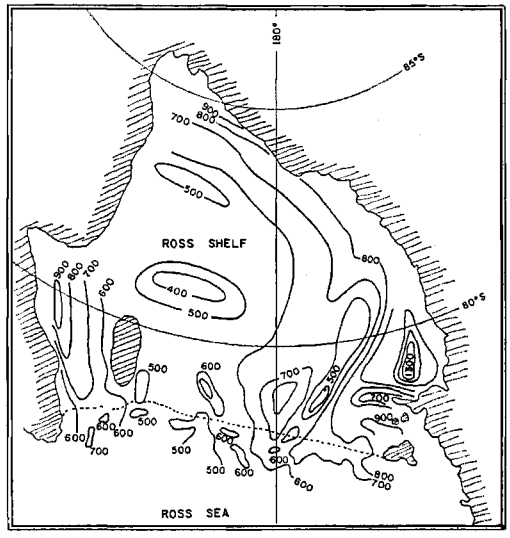

FIG. 9. *Depth of Water Below Sea Level in Meters.*

water for considerable distances into the mountain area.

Victoria Land

The Victoria Land plateau area proved more difficult to explore by seismic soundings than the low-elevation shelf areas. Deeper holes for explosives and various recording techniques were tried and to some extent were successful. To supplement the

reflection soundings, several refraction profiles were made.

During the 350 nautical miles traveled into the plateau area, no mountain ranges or nunataks were observed. The surface was characterized by quite rough sastrugi (see *Bulletin No. 22*).

Figure 10A shows the profile of the 1958–59 traverse from the Ross Ice Shelf through the Skelton inlet and glacier and into the plateau area, giving approximate surface elevations and ice thicknesses. At the western end of the line, near 130°E, the elevation of the surface was found to be about 2850 meters, comparable with the elevation at the South Pole Station. It is noted also that the surface elevation rises toward the west. The USSR-IGY Vostok Station, with an elevation of about 3420 meters, lies about 300 nautical miles farther west. This would

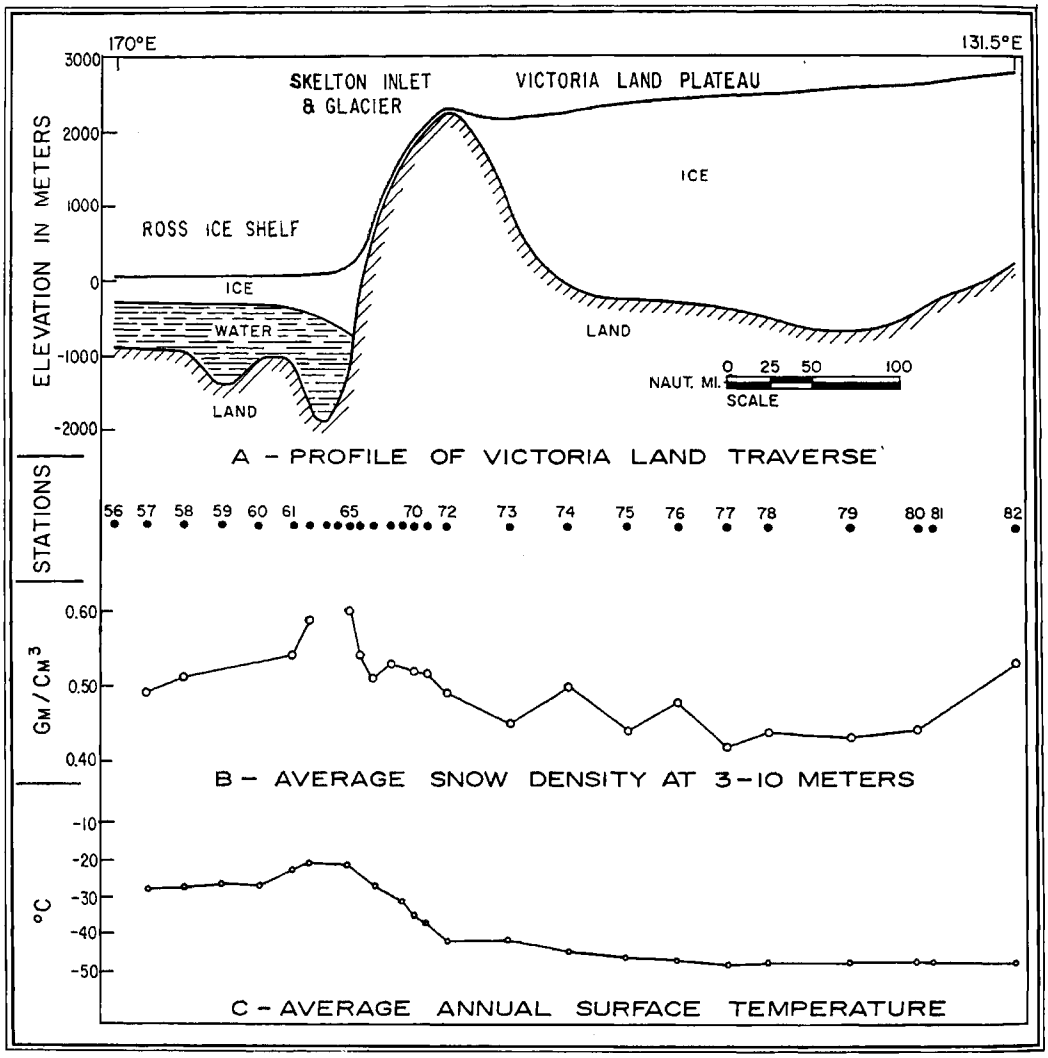

FIG. 10. *Profile from Ross Ice Shelf Westward into Victoria Land Plateau, Showing Surface Elevations, Ice Thickness and Bedrock Topography. Also shown are snow densities and temperatures. The gap in the center segment at Stations 63 and 64 reflects densities greater than 0.8, beyond the scale of the chart. Temperatures were taken at 10-meter depths; experience shows that these approximate average annual air temperatures just above the snow surface.*

require an average climb of 2 meters per nautical mile, or somewhat less than the slope observed at the end of the traverse.

Immediately west of the Skelton Glacier area, surface elevations drop about 150 meters, making it appear likely that drainage of plateau ice through the mountains along the western border of the Ross Ice Shelf is not significant. This is further substantiated by shelf thicknesses shown in Figure 8.

In Figure 10B are plotted the average snow densities between depths of 3 and 10 meters, as found in cores obtained during drilling of seismic shot holes. A significant density increase occurred in the Skelton Glacier area. At Stations 63 and 64, the surface consisted of hard, blue ice with a density greater than 0.8. On the plateau, the densities were generally low but quite erratic, an abnormally high value of .53 being found at the westernmost station.

Figure 10C gives the temperatures at a depth of 10 meters for the profile from the Ross Ice Shelf to the plateau area. (These are quite close to the average annual air temperatures near the snow surface; hence, they represent general climatic conditions.) From an average of —28°C (about —18°F) on the shelf, temperatures fell to —48°C (about —54°F) on the western part of the plateau line. This is not much different from the —50°C at the South Pole Station, more than 700 nautical miles farther south. The rise in temperature in the Skelton Inlet may reflect higher summer temperatures owing to exposed rock areas, or higher winter temperatures resulting from high average down-glacier wind speeds.

During the descent of the Skelton Glacier on the return trip, detailed altimetry was obtained by reading one of the altimeters at short time intervals while the vehicle was in motion. The figures were adjusted to

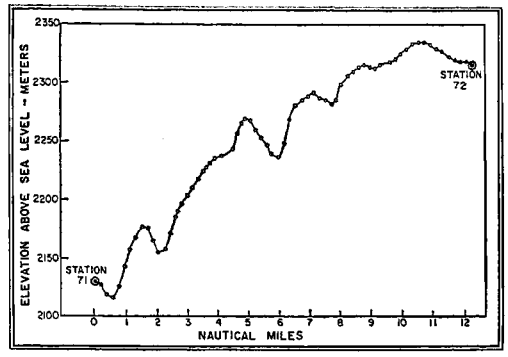

FIG. 11. *Elevations Near Top of Skelton Glacier. The altimetry readings on which these are based were taken during the descent of the glacier on the return trip.*

elevations at the major stations determined from multiple altimetry and transit surveys. Figure 11 shows part of the results of this study near the top of the Skelton Glacier, where the long ridges and troughs were quite pronounced.

An estimate of the average annual snow accumulation on the plateau is not yet available, and preliminary analyses indicate that snow characteristics as obtained from the pit studies may be quite difficult to interpret. If snow accumulation is small and wind erosion high, the changes in oxygen-isotope ratio with season may also be poorly defined. (See *Bulletin No. 21* for a discussion of oxygen-isotope methods.) For reliable information on accumulation patterns, it may be necessary to await future repeat observations of the snow stakes placed on the plateau during this traverse.

Future traverse parties from Scott Base will continue the exploration on the Victoria Land plateau, possibly tying in with French traverse work to the northwest and the USSR work to the west. The combined results will assist in the compilation of a comprehensive picture of this part of the Antarctic continent.

Hydrobiological Measurements on IGY Drifting Station Bravo

The following report is based on material supplied by Spencer Apollonio, Yale University. The IGY work it describes was supported by the Air Force Cambridge Research Center and the Woods Hole Oceanographic Institution.

As part of the IGY program, measurements were made at IGY Drifting Station Bravo, on Fletcher's Ice Island (T-3), to determine the level of primary organic productivity in the Arctic Ocean.

The productivity of the smaller plant and animal life in the sea is important in assessing potential marine food supplies, since fish resources depend on these lower forms of marine life for sustenance. Organic productivity can be determined by measuring the amount of photosynthesis taking place and the concentrations of chlorophyll in the water. The Station Bravo productivity studies included both of these measurements, and also determination of nutrient concentrations.

When the measurements were begun, there was little doubt that productivity would be low because of the unfavorable conditions for life in the Arctic Ocean. Nevertheless, it was hoped that the level could be determined quantitatively, and to some extent this has been achieved, although difficult working conditions made it impossible to accomplish some of the planned measurements.

Complete analysis of the plant and animal collections will take considerable time and the results will be reported later. Advice and assistance were received from J. H. Ryther, C. S. Yentsch, R. A. Vaccaro, and N. W. Corwin. J. A. Murray, Jr. supplied radiation data from Station Bravo observations.

Environmental Conditions

The drift of Station Bravo during this study was along the edge of the continental shelf, within 100 miles of the north coast of the Canadian Arctic Archipelago (see *Bulletin No. 24*). The ice island itself is estimated to be about 160 feet thick. Within a mile of the island the pack-ice thickness, determined from numerous corings, ranged from 10 to 30 feet in an apparently irregular manner. Beyond a mile from the island's edge, the pack ice was extremely broken and no thickness measurements were made.

The hydrobiological sampling site was on the pack ice about 500 feet from the edge of the island. Observations were made through a hole 14 feet in depth.

Hard, windpacked snow covers the ice from late August until about the first week of July. The melt curve for the snow cover of 1957 is shown in Fig. 12. It is probable that during the summer the snow cover is the greatest limiting factor on productivity in the ocean. No light-extinction coefficients are available for the various states of the snow. In April, however, under bright, clear conditions, light penetration was not detectable by a photocell and micro-ammeter at a depth of four inches below the snow surface.

During the summer snow-free period, extensive melt-water lakes cover the pack ice. Preliminary evidence from IGY Drifting Station Alpha (on an ice floe elsewhere in the Arctic Ocean) indicates that these lakes may act as lenses, concentrating light through the ice and increasing organic productivity below them.

Through the summer of 1957, a lead (long, narrow passage in pack ice) about 50 feet wide and 3–4 miles long persisted at a distance of 1½ miles from the sampling

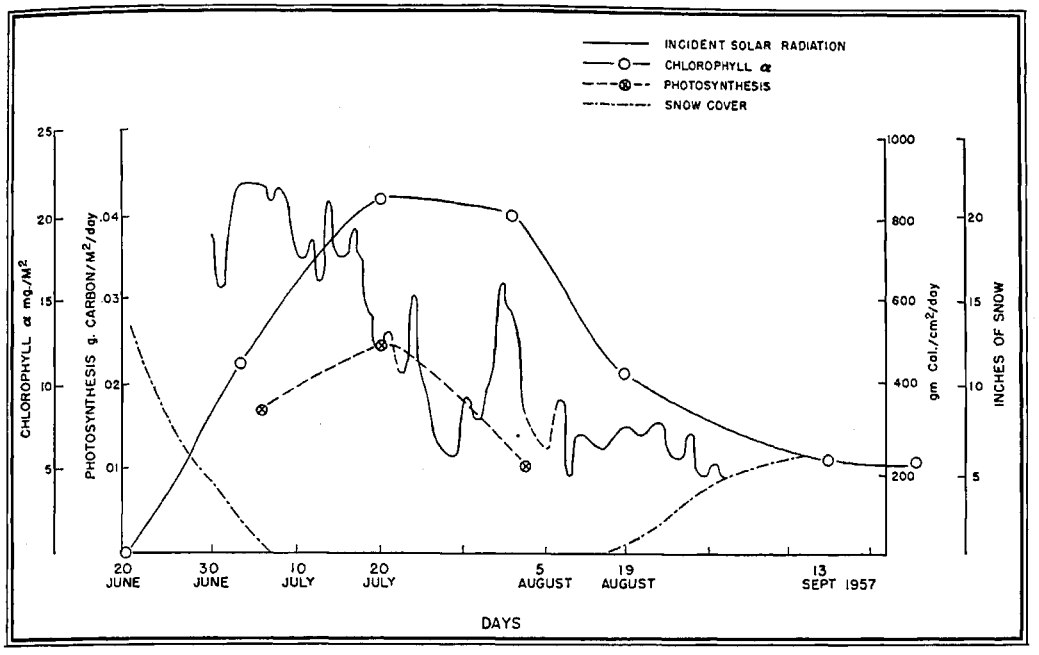

FIG. 12. *Average Thickness of Snow Cover and Average Amounts of Incident Solar Radiation, Photosynthesis, and Chlorophyll α, Summer 1957, at IGY Drifting.*

site. The possible existence of other leads close to the island, or the amount of open water in that part of the ocean, is not known. Visual observations on five aircraft flights to Station Bravo, however, suggest that open water occupies less than 1% of this area in summer. Hence, the effect of ice-free, open water on the results of this study can be considered negligible.

It is significant that patches of diatoms (microscopic algae) frozen in pack ice in the Arctic Ocean, mentioned by Nansen in 1902, and by others, were never noticed in the vicinity of Station Bravo. It is also remarkable that invertebrate animals were never seen, either in the sampling hole or in the lead. Efforts to trap amphipods (small crustaceans) by methods that had proved successful in other parts of the Arctic Ocean were fruitless. One seal was seen in the lead.

Photosynthesis Measurements

During June, July, and August 1957, net photosynthesis (photosynthesis minus respiration) of the phytoplankton—floating plant life—was measured at five locations by the carbon-14 method. (It seems obvious that photosynthetic carbon assimilation is impossible during the winter in higher Arctic latitudes owing to the lack of light during the six-month-long Arctic night.) Water samples were collected by non-metallic samplers. One milliliter of $C^{14}O_3^=$ (activity 2,400,000 counts/min) was added to each sample in a 150-milliliter glass-stoppered bottle and the bottle resuspended for 24 hours at the depth from which the sample was taken. The samples then were filtered through millipore filters; these filters were preserved and the amount of activity later determined at the Woods Hole Oceanographic Institution.

For samples taken at the first two locations, on June 12 and 21, no photosynthesis could be detected by this sensitive technique. Photosynthesis was detected at the other three locations, on July 6, July 12, and August 7.

A maximum rate of 0.024 $gC/m^2/day$ in

the upper 100 meters of the sea, a very low rate of photosynthesis, was detected for July 21. (P. T. Marshall and E. Steeman Nielsen, separately, have reported a maximum net photosynthetic rate in sub-Arctic waters of about 1 $gC/m^2/day$, about 40 times the above rate for the Arctic Ocean.) The average of the three stations at which photosynthesis could be detected was 0.017 $gC/m^2/day$. For the period June 20-August 20, the daily average was 0.01 gC/m^2.

If it is assumed that measureable net photosynthesis takes place in the Arctic Ocean only during this 60-day period, the total yearly net primary productivity is about 0.6 gC/m^2. Assuming, also, that the Station Bravo data are representative of the entire Arctic Ocean, the total annual net photosynthetic carbon production is computed at 8.45×10^6 tons. The annual net production for all oceans has been estimated by Steeman Nielsen and E. Aabye Jensen at 1.5×10^{10} tons.

Chlorophyll Concentrations

Water samples were collected and filtered through millipore filters; these filters were preserved and analyzed at Woods Hole for chlorophyll concentrations. The maximum of 0.37 mg/m^3 on August 5, 1957, measured just under the ice, compares closely with the August maximum of 0.4 mg/m^3 found two decades earlier in the upper 20 meters of the Arctic Ocean by the Soviet investigator Shirshov.

It appears from comparisons with similar studies in other Arctic areas that ice-free Arctic waters may develop a maximum chlorophyll concentration as much as 13 times that found in the ice-covered Arctic Ocean. The average concentration in these ice-free waters during one season may vary from 2 to 5 times that of the ice-covered areas. It is significant, however, that even at a depth of 500 meters in the Station Bravo area some chlorophyll could be detected during the summer.

Nutrients

Although there seems little doubt that phytoplankton development under the Arctic Ocean ice pack is limited primarily by light conditions, examination of the phosphate and nitrate concentrations of the water is of interest with regard to potential plant growth. From expected carbon-nitrate-phosphate ratios of the plankton it is possible to calculate the total potential amount of productivity that might occur if nutrients were the only factors limiting growth and if they were not being replenished to the water.

Several profiles of nitrate and phosphate concentrations were obtained from October 1957 through May 1958. Maxima of both nutrients occurred characteristically at a depth of about 125 meters. Phosphate concentrations were quite constant below 200 meters, but nitrate concentrations were more variable below this depth. Minimum values of both nitrates and phosphates were found in the upper few meters, and at times nitrates were not detectable at all in the upper levels. Secondary maxima generally existed between depths of 350 and

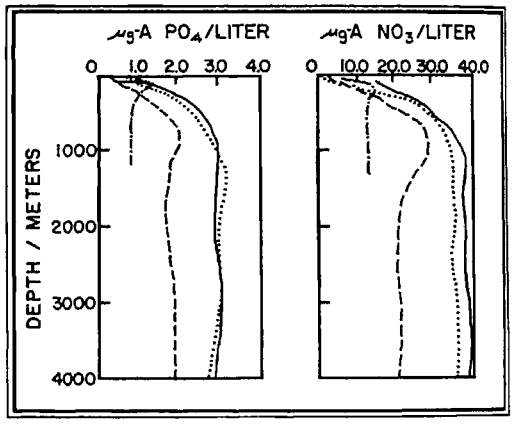

FIG. 13. *Phosphate and Nitrate Concentrations in the Arctic Ocean (dot-dash line) Compared with Concentrations in the Indian Ocean (solid line), Pacific Ocean (dotted line), and Atlantic Ocean (dashed line). Concentrations are shown in microgram atoms (μg·A) per liter.*

450 meters, and on two dates the nitrate values were slightly higher in this interval than at 125 meters. The secondary phosphate maxima were much less pronounced than those of the nitrates.

The usual oceanic ratio of nitrogen to phosphorus, 16:1 by atoms, was not regularly observed. In the upper 150 meters, the observed ratios were quite low (5:1 and 9:1), and below 200 meters ratios were higher than expected (17:1 and 27:1). The general distribution of the ratios was somewhat variable. Comparisons of inorganic phosphate data and data on total phosphorus show that at all depths some organic phosphorus exists, dissolved and/or in particles. Figure 13 compares graphically the nitrate and phosphate concentrations of the Arctic Ocean with those of other oceans.

Total phosphorus values from Station Bravo are similar to those reported from the Soviet pre-IGY drifting station, NP-2; data from US-IGY Drifting Station Alpha show the same pattern. (See *Bulletin No. 24* for information about the drift path of Station Alpha and reference to material on its scientific programs.)

Two profiles of nitrate concentrations were taken through the pack ice. No detectable phosphate concentrations were found, however.

Conclusions

From IGY and pre-IGY studies in Arctic and other waters, it appears that the Arctic Ocean, although comprising 1/23 the area of all oceans, contributes only about 1/1000 of the total oceanic production of small plant and animal life.

Even if the paucity of sunlight penetrating the Arctic ice pack did not limit phytoplankton growth, the poverty of the Arctic Ocean in nitrate and phosphate nutrients would still make its productivity level one of the lowest in the world.

IGY Bibliographic Notes

This is the fourteenth of a series of bibliographic notes on IGY programs and findings. The references are selected largely from an IGY bibliography under preparation in the Science and Technology Division of the Library of Congress

IGY Bibliography

The first volume of the International Geophysical Year Bibliography is available from the Publishing and Printing Office, National Academy of Sciences, 2101 Constitution Avenue, N. W., Washington 25, D. C. Price $1.00, postage prepaid. The 64-page volume contains 704 references.

The Bibliography is being compiled at the Library of Congress and is a joint project of the Library, the Academy, and the National Science Foundation.

S. K. Chakrabarty: Cosmic Ray Work at the Bengal Engineering College, Howrah. *Journal of Scientific and Industrial Research,* Vol. 17A, no. 12. Dec. 1958. Pp. 81–82. Diagr.

M. W. Chiplonkar, R. N. Karekar, T. A. Raju, and M. S. Hattiangadi: A Preliminary Report "On the Nature and Origin of Atmospherics." *Journal of Scientific and Industrial Research.* New Delhi, India. Vol. 17A, no. 12, Dec. 1958. Pp. 3–23. Diagr., refs.

Herbert Friedman: Rocket Observations of the Ionosphere. *Proceedings of the IRE.* Vol. 47, no. 2. Feb. 1959. Pp. 272–280. Diagr.

Roger M. Gallet: The Very-Low-Frequency Emissions Generated in the Earth's Exosphere. *Proceedings of the IRE.* Vol. 47. Feb. 1959. Pp. 211–231. Illus., diagr.

E. I. Gal'perin, A. V. Goriachev, and S. M. Zerev: Crustal Structure Researches in the Transition Region from the Asiatic Continent to the Pacific. (In Russian). *Izd-vo Akademii Nauk SSR.* 28 pp. Diagr., maps.

I. Harris and R. Jastrow: *Demise of Satellites 1957 Alpha and 1957 Beta.* Washington, Naval Research Laboratory. 1958. Miscellaneous Paper No. 165.

R. A. Helliwell and M. G. Morgan: Atmospheric Whistlers. *Proceedings of the IRE.* Vol. 47, no. 2. Feb. 1959. Pp. 200–208. Illus., diagr., map.

The International Geophysical Year and Space Research. U. S. Congress. House of Representatives. *Staff Report of the Select Committee on Astronautics and Space Research.* Washington, Government Printing Office. 1959. 36 pp.

J. B. Kalinin: Soviet Investigation of Geomagnetism. (In Russian). *Priroda.* No. 8. Aug. 1958. Pp. 50–55. Diagr., maps.

D. C. King-Hele: Density of the Atmosphere at Heights between 22 KM. and 400 KM. from Analysis of Artificial Satellite Orbits. *Nature.* Vol. 183, no. 4670. May 2, 1959. Pp. 1224–1227. Diagr.

K. M. Kotadia: Meteors and E_s Ionization. *Journal of Scientific and Industrial Research.* Vol. 17A, No. 12. Dec. 1958. Pp. 46–49. Diagr.

M. G. Krishnamurthi, G. Sivarama Sastry, and T. Seshagiri Rao.: Radio Emission from the Sun at 30 MC/S. *Journal of Scientific and Industrial Research,* Vol. 17A, no. 12. Dec. 1958. Pp. 71–73. Refs.

La Fusée Lunaire Expérimentale à Satellite: Pioneer I. *Fusée et Recherche Aeronautique.* Vol. 3, No. 3. 1958. Pp. 119–122. Illus., diagr.

E. M. Lin'kov: Study of the Elastic Properties of Ice Cover in the Arctic. (In Russian). *Vestnik Leningradskogo Universiteta.* No. 4. *Seriia Fiziki i Khmii.* No. 1. 1958. Pp. 17–22. Diagr.

Ludwik Liszka: A Type of Variation of the Signal Strength from 1958 δ 2 (Sputnik 3). *Nature.* Vol. 183, no. 4672. May 16, 1959. Pp. 1383–1384. Diagr.

George H. Ludwig: Cosmic-Ray Instrumentation in the First U. S. Earth Satellite. *Review of Scientific Instruments.* Vol. 30. April 1959. Pp. 223–229. Illus., diagr.

S. L. Malurkar: Geomagnetic Work at Albag, Annamalainagar and Trivandrum during the IGY. *Journal of Scientific and Industrial Research.* Vol. 17A, no. 12. Dec. 1958. Pp. 33–35. Refs.

D. F. Martyn: The Normal F Region of the Ionosphere. *Proceedings of the IRE.* Vol. 47. Feb. 1959. Pp. 147–155. Diagr.

W. G. Metcalf: Oceanographic Data from Crawford Cruise 16, Oct. 1–Dec. 11, for the International Geophysical Year. *Woods Hole Oceanographic Institution.* June 1958. 127 pp. Diagr., map. Reference No. 38–31.

G. R. Miczaika and E. W. Wahl: *The Orbital Motion of the Earth Satellite 1957 β from April 1 to its Decay April 14, 1958.* Bedford, Mass., Air Force Cambridge Research Center. June 5, 1958. 38 pp. Diagr., maps.

A. P. Mitra, K. A. Sarada, N. V. G. Sarma, and M. N. Joshi: Radio Patrol of Solar Flares. *Journal of Scientific and Industrial Research.* Vol. 17A, no. 12. Dec. 1958. Pp. 74–80. Illus., diagr.

B. Mongin: Les Terres Australes et Antarctiques Françaises. *Forces Aériennes Françaises.* Vol. 13, no. 144. Jan. 1959. Pp. 83–104. Illus., maps.

Benjamin Nichols: Auroral Ionization and Magnetic Disturbances. *Proceedings of the IRE.* Vol. 47. Feb. 1959. Pp. 245–254. Diagr.

M. M. Nita: On the Motion of Artificial Satellites Taking into Account the Resistance of the Medium. *Revue de Mécanique Appliquée.* Vol. 3, no. 1. 1958. Pp. 57–76. Diagr.

Programme of IGY Solar Observations in India. *Journal of Scientific and Industrial Research.* Vol. 17A, no. 12. Dec. 1958. Pp. 68–69. Refs.

B. Ramachamara Rao and D. Satyanarayana Murty: A New Continuous Wave Radio Method for the Study of Ionospheric Drifts. *Journal of Scientific and Industrial Research.* Vol. 17A, no. 12. Dec. 1958. Pp. 63–67. Diagr., refs.

Report of the Bureau of the Advisory Council for the IGY (Otchet biuro SK MGG). *Informatsionnyi Biulleten' Mezhdunarodnogo Geofizicheski. Goda.* No. 4. 1958. Pp. 3–7.

R. Sethuraman: Rates of Fading of Reflected Pulses of Vertically Incident Electromagnetic Waves at Ahmedabad on 2.6 and 4.0 MC/S. *Journal of Scientific and Industrial Research.* Vol. 17A, no. 12. Dec. 1958. Pp. 50–53. Diagr., refs.